FOREWORD

This report was prepared by the Institute of Engineering Research, University of California at Berkeley, California, under USAF Contract AF(313)-6630. The contract was initiated under Project 7360 "Materials Analysis and Evaluation Techniques", Task No. 736001, "Thermodynamics and Heat Transfer". It was administered under the direction of the Directorate of Materials and Processes, Deputy for Technology, Aeronautical Systems Division with Mr. Robert A. Winn acting as project engineer.

Part I of this report covered the work conducted from the time of project initiation in July 1959 to September 1960 and this Part II covers the period from September 1960 to December 1961. This research was conducted under the direction of R. A. Seban, Professor of Mechanical Engineering, principal investigator, and R. E. Rolling, research engineer. Grateful acknowledgement is accorded for the assistance of R. Eberhart, E. Anderson, and D. Russell.

ABSTRACT

Results obtained for the spectral emittance of materials measured in air at intermediate temperatures of about 1400°F are compared to the spectral reflectances measured at room temperature to provide an appraisal of the effect of temperature on those radiation properties. The temperature effect is found to be small for oxidized metals and for ceramic coatings and some of the apparent effects are still associated with variation of the material and with inaccuracy of measurement. Spectral emittances for metals were determined only for platinum; these results and those of other investigators are analyzed to show that the apparent coincidence in the applicability of the Hagen-Rubens equation is of increased validity at higher temperatures and that this is the basis for the applicability of that formulation to the specification of the total emittance.

A system designed for the determination of the spectral emittance of metals or of materials with metallic substrates, in vacuum or in an inert atmosphere, is described and preliminary results are indicated for Inconel.

Spectral and total properties of various materials obtained in certain tasks are also presented, this comprising particularly the properties of ceramic coatings prepared by the Chance-Vought Company.

PUBLICATION REVIEW

This report has been reviewed and is approved.

FOR THE COMMANDER:

R. E. Brocklehurst

ROBERT E. BROCKLEHURST
Technical Director
Physics Laboratory
Directorate of Materials
and Processes

TABLE OF CONTENTS

LIST OF FIGURES

LIST OF FIGURES (CONTINUED)

I

INTRODUCTION

The first part of this report [1] presented thermal radiation properties of a number of materials and also described the systems by means of which these properties were obtained. The properties were, in general, normal values only, and comprised the spectral reflectance from 0.30 to 25 microns, of the material at room temperature; the spectral reflectance, from 1 to 25 microns, of the material at a temperature of 1000°F; and the total emittance for temperatures from 500°F to 2500°F, all being measured in air. Spectral properties at higher temperatures are best determined as emittances and there was described a system for spectral normal emittance determinations in which the sample was in air and with which temperatures up to 1800°F could be obtained. At that time only a few results were available from this system and for oxidized nickel alloys these indicated, for most of the range from 2 to 15 microns, a correspondence between the reflectance deduced from the emittance measured at high temperature and the reflectance measured at room temperature. This corroborated, relatively, the results found for the reflectance of oxidized and coated materials at 1000°F, which were only slightly different from those measured at room temperature, but which did depart from them sufficiently so that the total emittance predicted from the spectral values measured at 1000°F turned out to be, for those good emitters, about 5% below the emittance predicted from the reflectance measured at room temperature. The measured total emittances, moreover, were closer to the prediction made from the room temperature reflectance than from the prediction based on the reflectance measured at high temperature.

Additional results for the spectral emittance at temperatures between 1200°F and 1800°F are given here. Because of the air environment in which the sample was situated, these results are limited to oxidized and to coated metals, and for polished platinum. Clearly the elimination of oxidation effects requires measurements in an inert atmosphere or in a vacuum and the system from which the results were obtained was an interim device to the closed system which was developed subsequently and which is described in Section 4. The results from this unit are still preliminary and are not reported except as they appear in Section 4.

Manuscript released for publication 31 January 1962 as a WADD Technical Report.

The results for the spectral emittance of oxidized and coated materials are compared in Section 2 to the results for the reflectance at room temperature. While these comparisons are still affected by variability in the material itself, the indication of the comparison is one of relatively small effects of temperature on the spectral properties of these dielectric surfaces. The differences that do exist occur in the long wave length region, so that they exert but a small influence on the total emittance at high temperatures.

The effect of temperature on the spectral emittance of metals is considered in Section 3, in reference to the results obtained for platinum and to available results for nickel. A review of the electromagnetic theory and the contribution of photoelectric effects is combined with the available results in an examination of the reliability of the often specified Hagen-Rubens relation for the specification of the emittance of metals, to indicate that its applicability is due apparently to a coincidence of effects. Results for the effect of surface stress on the reflectance at room temperature are presented also to indicate that this effect also may provide correspondence with the Hagen-Rubens relation even for metals such as copper for which it would ordinarily be considered inappropriate.

II

TEMPERATURE EFFECTS ON THE REFLECTANCE OF COATED OR OXIDIZED METALS

2.1 Introduction

The thermal radiation properties of metals coated with refractory materials and of metals with well oxidized surfaces are determined by the properties of these surface layers. These layers are essentially dielectric, with optical properties determined by oscillators associated with electronic, ionic, and molecular vibrations. Except near these resonance frequencies, the absorption tends to be low and the index of refraction relatively invariable and some of the absorption of these layers arises also from the irregularity of the surface and from internal interfaces which diminish the transmission through multiple reflection and scattering. In broad spectral regions the reflectance of the material is low and relatively constant, as is expected for a dielectric.

The temperature dependence of the radiation properties of such materials is usually presumed to be small, a view of course guided by the low reflectance of these materials in general, so that even a significant change in the reflectance affects very little the total emittance of the material. This latter effect, of course, has been demonstrated by the fair predictions of total emittance at elevated temperatures that are produced from the reflectance measured at low temperature. A more direct assessment is naturally obtained by the measurement of spectral properties at higher temperature, and reflectances have been measured for numerous materials of the type under consideration, as reported previously[1] and here after described. These however, were scarcely sufficiently definitive, other than indicating that temperature effects were small. Since the temperature at which reflectance could be determined was limited to the order of 1000°F, studies of the effect of higher temperatures on the spectral properties required the measurement of spectral emittance. Such measurements were made, in air, with sample temperatures in the temperature range from 1200°F to 1800°F, using a system previously described. The results therefrom are the major presentation of this section and these support the relative invariability of the spectral properties with the temperature, though they do show local variations which are moreover still made uncertain by the question of the stability of the material with respect to further oxidation during the period of measurement.

Finally, there is presented a brief consideration of the effect on the optical constants that would be due to band broadening in a single classical oscillator. On the inference that an increase in band width might accompany an increase in temperature, these results do support some of the local effects of temperature that are demonstrated by the results. But such correspondence as does exist is at present insufficient to support fundamentally the assumption of band broadening that is involved.

2.2 Reflectance at Elevated Temperatures

The heated cavity reflectometer can be operated with elevated sample temperatures by decreasing the amount of sample cooling, as previously described[1]. The radiation detected is then composed of both reflection and emission and the latter contribution must be subtracted appropriately in terms of the measured temperature of the sample. As the sample temperature increases the portion of the detector response that is due to reflection diminishes and a sample temperature of 1000°F is the practical limit for a cavity temperature of about 1400°F. The determination of the sample temperatures is critical and an error of 10°F produces errors of 10% in the reflectance for a material having a reflectance of 0.20. This error diminishes at wave lengths below 4 microns and better results are achieved at short wave lengths. The temperature, measured by a thermocouple welded to the metallic substrate at the cooled side of the sample, tends to be lower than that of the surface layer, so that the contribution of the emission tends to be deficiently appraised, yielding a situation in which the indicated reflectance tends to be too high.

The reflectances that were obtained at a temperature of 1000°F either coincided closely with the reflectance measured at room temperature or were higher at wave lengths below about 8 microns and at longer wave lengths were slightly below the values measured at room temperature. Since it is the reflectance at shorter wave lengths that makes the significant contribution to total values at high temperature, a lower total emittance was predicted from the reflectances measured at high temperature than was predicted from the reflectances measured at room temperature. The experimental values of total emittance showed the opposite behavior and this casts doubt on the higher spectral reflectances found at short wave lengths with a hot sample. The spectral emittance results which follow imply also that the two reflectances should have been more nearly the same in the short wave length region.

2.3 Emittance at Elevated Temperature

As an intermediate step to the construction of the system which is described in Section 4 for the determination of spectral emittances at high temperature in an inert atmosphere, there was developed a system for operation in air at temperatures up to about 1800°F and this system has been described[1]. Basically, it is comprised of a heated cavity and of a sample heating furnace for heating the sample by irradiation on the side opposite to that observed. A mirror system permits observation of either the cavity or the sample through the same set of optics and the emittance is determined from the detector response in the two observations together with the observed temperatures of the cavity and of the sample. The major error in the emittance so determined is associated with the measurement of sample temperature and an error, ΔT, in this determination (or, more specifically, an aggregate error of ΔT in the temperature of sample and cavity), produces an error in the emittance of $\frac{\Delta \epsilon}{\epsilon} = \frac{25800}{\lambda} \frac{\Delta T}{T^2}$. This is serious at short wave lengths and renders quite questionable the results at wave lengths below 2 microns when the operating temperature is of the order of 1500°F. Since the temperature of the radiating layer on a coated sample tends to be below the measured substrate temperature, the emittances as determined are too low, and the inferred reflectances consequently tend to be high. Thus the trend of error due to temperature variation in the surface layer is the same as it is in the "heated" reflectance determinations, with a magnitude that depends on the conductivity and thickness of the surface layer. The actual nature of the emittance data obtained does suggest, however, that the thermocouple readings tended to be low and the emittance as evaluated was probably above rather than below the true value.

In the desire to maximize the temperature uniformity in the region of observation, the original design of the spectral emittance unit required samples 1-7/8 inches in diameter. Thus, when a reflectance determination was desired after an emittance measurement, a 7/8 inch diameter reflectance sample had to be cut from the center of the emittance sample. To achieve an optimum comparison this was done for all the cases here reported but this requirement limited to one the comparisons between reflectance and emittance that could be achieved. Later examination showed that 7/8 inch diameter samples could be used in the emittance unit but this change was not made early enough to be of profit in the group of measurements presented here.

Results are presented for the nickel alloys M252, Rene 41, and Inconel, and for the material HS25, all of which had oxide layers which appeared to be relatively stable in respect to

temperature cycles below 1800°F. In addition, results are shown for Stainless Steel A286, with which however the oxidation was progressive, and for certain coated samples with a molybdenum substrate, obtained from the Chance-Vought Co. The results are indicated as reflectances, one being unity minus the emittance measured at high temperature, and the other the reflectance determined from the same sample at room temperature after the emittance determination was completed.

Oxidized Nickel Alloys

Figure 1 presents the results for oxidized Inconel and includes a curve for the low temperature reflectivity reported before[1]. The present results agree fairly with earlier values, though there is separate evidence of considerable difference in the spectral properties of different Inconel samples. Except in the region of 9 microns, there is close correspondence between the reflectances at high and low temperature and from the experimental standpoint, there is for these results good overlap between the results obtained with the NaCl and KBr prisms, which are distinquished by different point designations on these and on the succeeding results.

The relative insensitivity to temperature of the reflectances shown on Figure 1 is at considerable variance with the previous results[1] for oxidized Inconel, which showed a substantial increase in reflectance at high temperature for short wave lengths.

Figure 2 shows the results for oxidized alloy M252, and this figure contains points only for emittance values, since oxidation had progressed so far in this sample when the emittance data were obtained that a suitable reflectance sample could not be cut from it. The low temperature values that are shown by the solid curve were obtained from a different sample of the same material but below 9 microns these values are practically identical to those deduced from the emittance, while at long wave lengths the reflectance that is deduced from the emittance is lower than the room temperature value. A dashed curve is shown for the reflectances measured at 1000°F and below 9 microns these are slightly above the low temperature values. If agreement is forced at short wave lengths then the agreement with the emittance results is improved at the long wave lengths. Only a small shift would be needed and the correspondence that is achieved is an illustration of the stability of the oxide on this material.

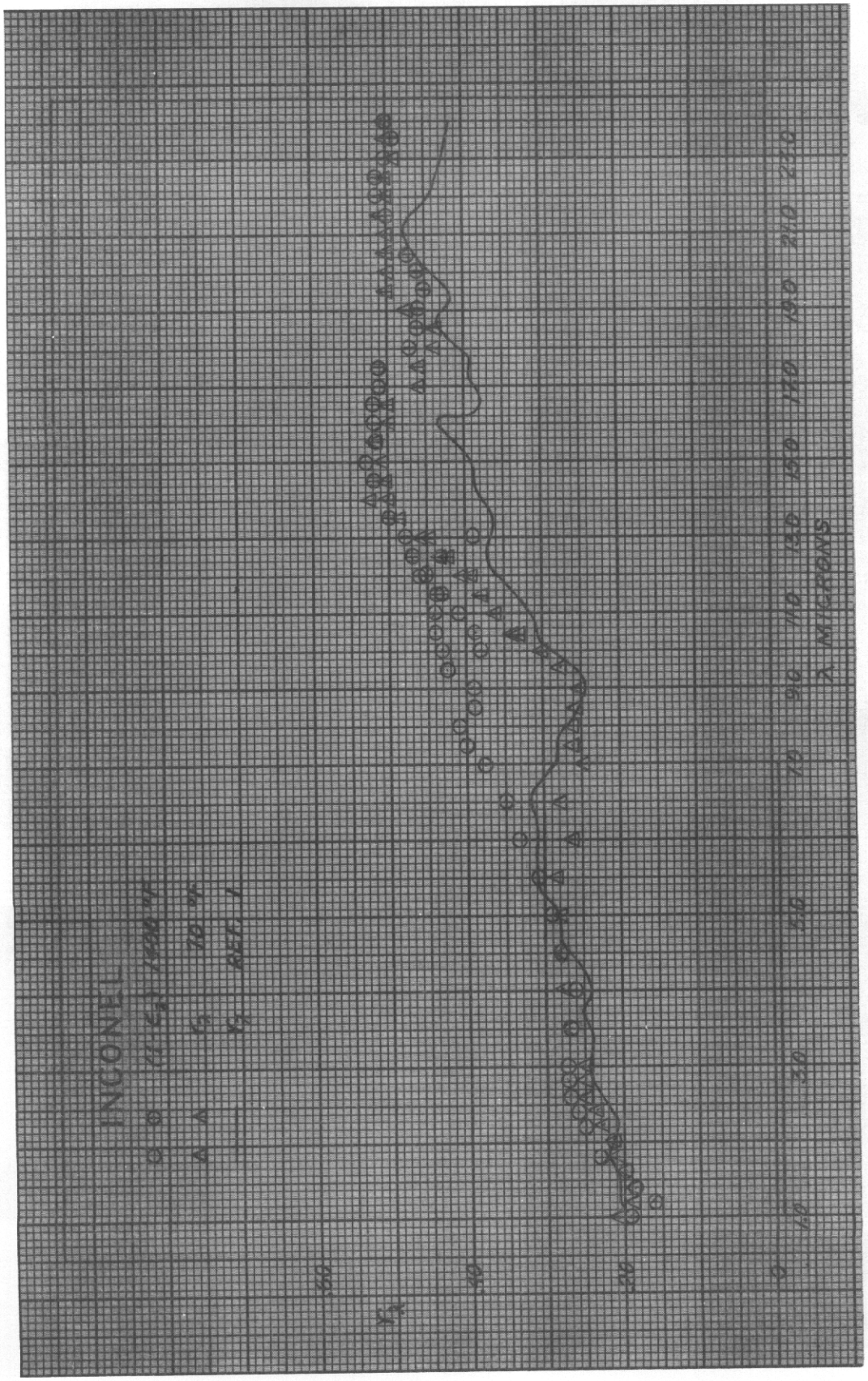

Fig. 1: Spectral Reflectance of Oxidized Inconel

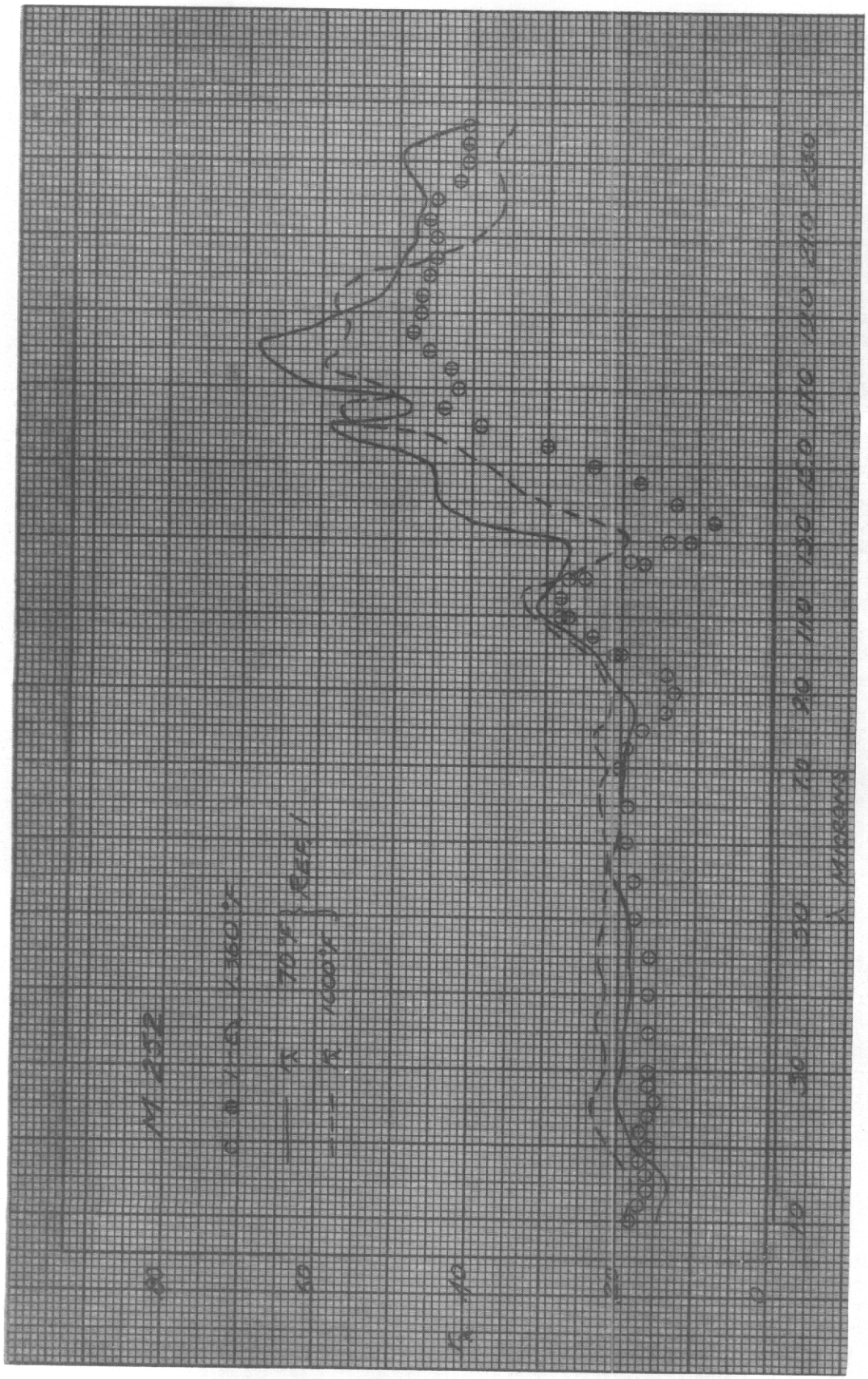

Fig. 2: Spectral Reflectance of Oxidized M 252

Figure 3 shows results for Rene 41 (Unitemp 41), a material almost the same as M252, but the results obtained with it do not show the same kind of agreement that is shown for the latter material on Figure 2. For this material, also, the reflectance at low temperature, shown by points, was obtained from the emittance sample and that reflectance is lower than the one shown by the solid curve of the earlier report. A different original specimen was involved and part of the difference indicates the variation that can be expected in the same material. The emittance and reflectance results, shown by points, agree fairly until about 5 microns, with the low temperature values becoming higher as the wave length increases. At long wave lengths this difference becomes substantial.

HS25 Cobalt Chromium Alloy

Figure 4 shows for this material a small influence of temperature on reflectance at wave lengths below 9 microns. There is a departure above this, and the low temperature reflectance is lower than the high temperature value that is deduced from the emittance determination. For wave lengths above 15 microns, where only the results from a different reflectance sample are available, there is a substantial change due to the change in temperature, with, on the average, a higher reflectance at elevated temperature.

Stainless Steel A286

Most of the results that are shown for this material on Figure 5 are not appropriate for an appraisal of the dependence of the reflectance on temperature, for the results obtained from the emittance, and shown by points on the figure, were derived from an originally unoxidized sample which oxidized progressively, before the first points were obtained, and thereafter as succeeding data were taken at various subsequent times. Thus the points reveal the effect of progressive oxidation but only those associated with the final operation can be interpreted as being representative of a well oxidized condition.

The solid curve represents the low temperature reflectance obtained from a well oxidized sample that was cut from another sample from which total emittance data were obtained and the dashed curve represents the deduction from spectral emittance measured on this sample. These comparable results do correspond well up to 8 microns; while at longer wave lengths the emittance is reduced. The higher temperature reflectances also agree fairly with those obtained from the first spectral emittance sample after the longest period of oxidation and there appears to be a definite reduction of the reflectance, at higher temperature, at wave lengths above 8 microns.

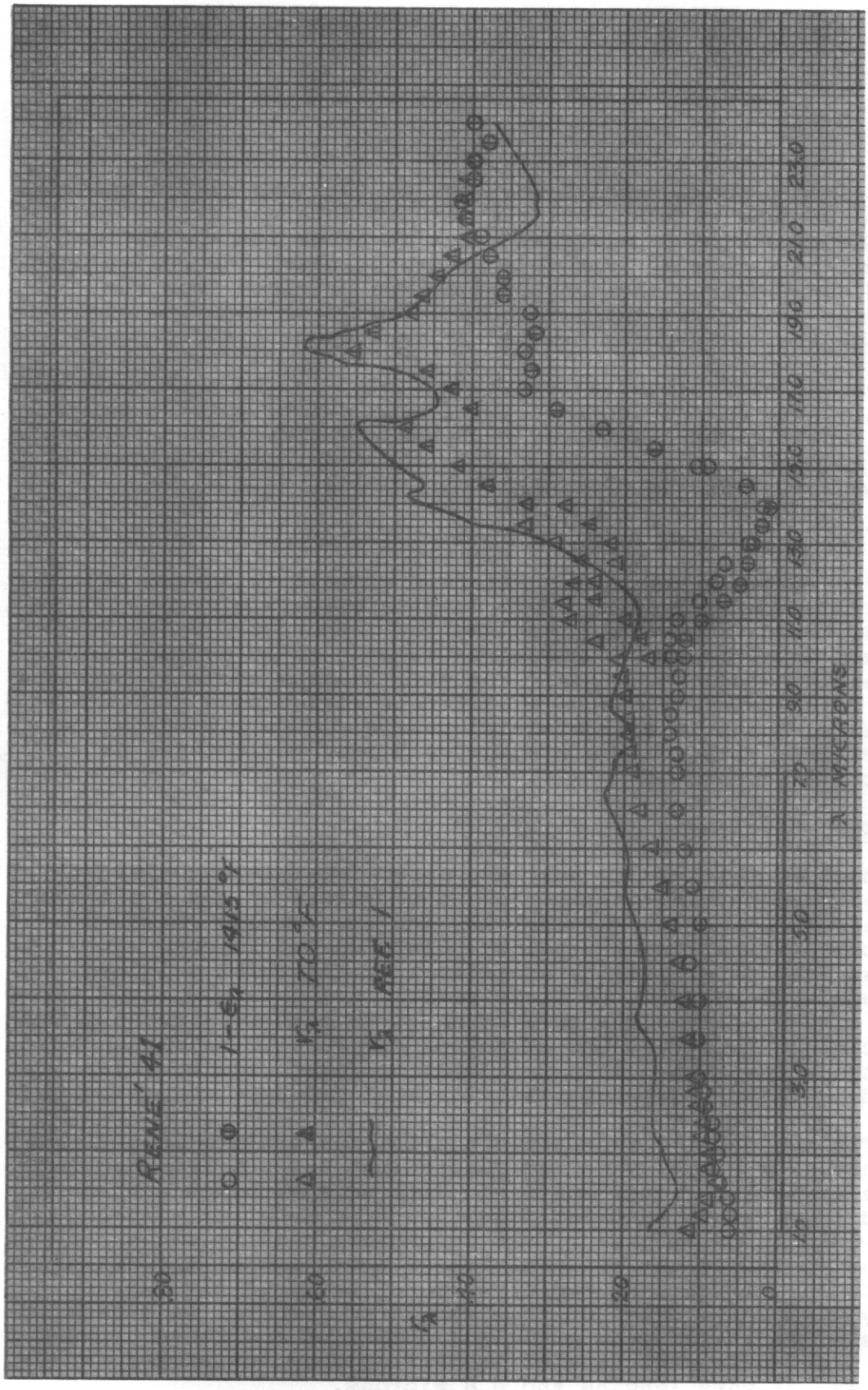

Fig. 3: Spectral Reflectance of Oxidized René 41

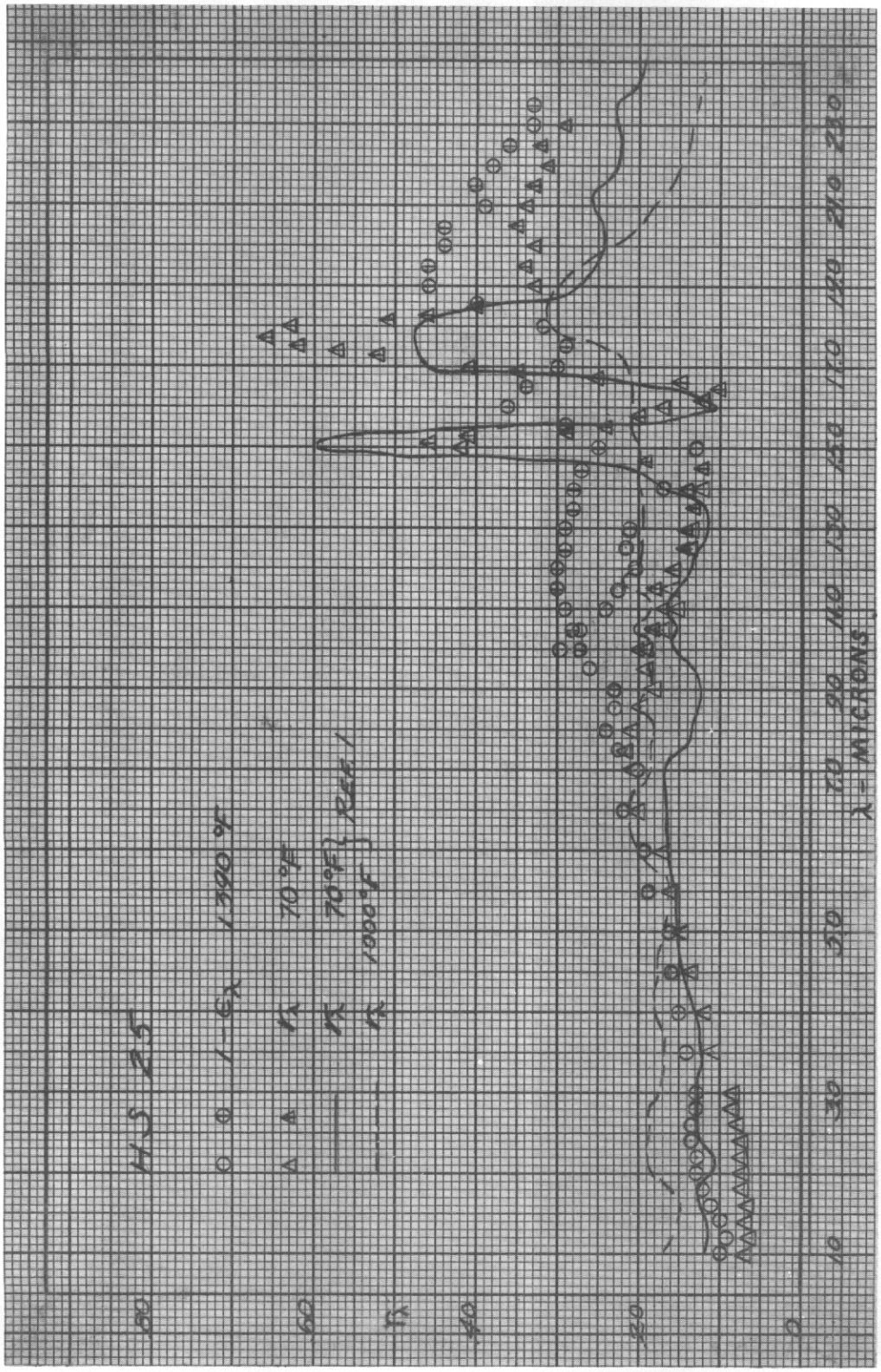

Fig. 4: Spectral Reflectance of Oxidized HS 25

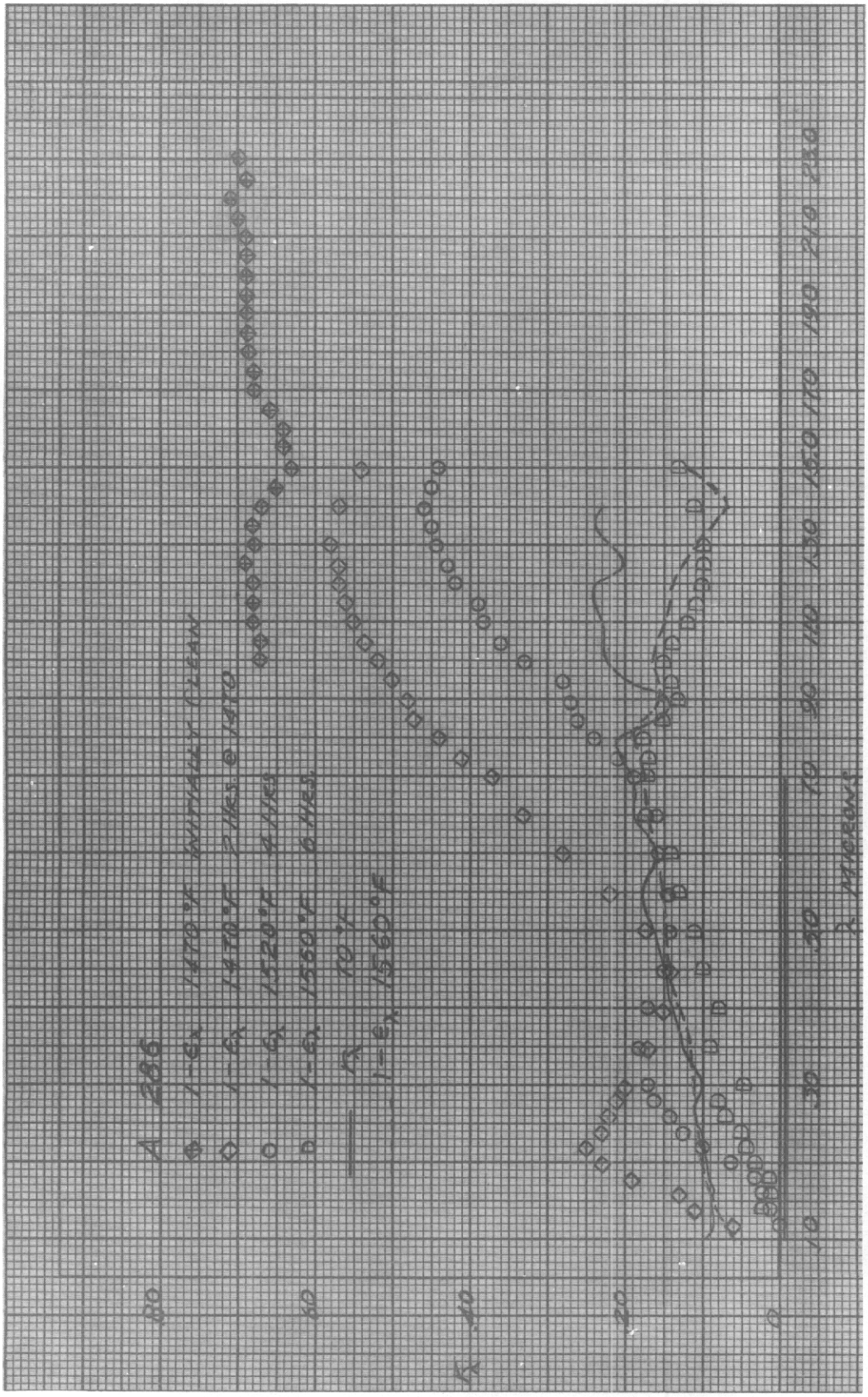

Fig. 5: Spectral Reflectance of Oxidized A 286 Stainless Steel

Chance-Vought Coated Materials

Part of the program on which this report is based involved the determination of spectral reflectances and emittances, and total emittances for certain coated molybdenum materials produced by the Chance-Vought Company. The ceramic coatings were intended to prevent oxidation of the substrate and the thermocouples attached to the substrate were coated in an effort to prevent oxidation at the point of attachment. Ideally, the relative stability of the coating should have provided results for low and high temperature reflectance which would focus quite directly on the effect of temperature on this property. Actually there existed a number of interfering factors, which are defined in detail in Section 5. The radiation properties of different samples of the same material were found to vary to some degree and the thermocouple attachments to the emittance samples failed despite the obvious care taken in making the attachment. The latter difficulty required thermocouple reattachment on the metallic substrate and the consequent oxidation problems then limited to about 1200°F the temperature at which the spectral emittance could be determined.

Figure 6 shows for the three types of coating involved, the reflectance at 1200°F as inferred from the emittance obtained at that temperature and the figure also shows the reflectance at room temperature as obtained from a reflectance sample cut from the larger sample after the spectral emittance had been determined. A third curve, a light dashed line, is shown to reveal that there existed an effect of aging despite the coating of the material and this curve is the room temperature reflectance obtained from the same sample after heating in air for one hour at 2000°F, subsequent to the first reflectance determination. Of course the edges of this 7/8 inch sample were bare after it had been cut from the emittance sample, but the evidence of the MoO_3 coating on the sample after this aging was such as to make it improbable that this oxide condensed from evaporation from the edges but rather originated from gas penetration through the coating. Similar treatment of a fully coated 7/8" diameter sample also led to similar results. What can be considered in support of the comparability of the basic reflectance curves of Figure 6 is that the emittance sample was never heated to much more than 1200°F and the aging of the sample after the first "cold" reflectance measurement was the first period of exposure to higher temperature.

The reflectances at low and high temperature for the material CV II + IX are practically the same below 6 microns, after which the high temperature reflectance is alternately below and above the low temperature value. Only at 12 microns

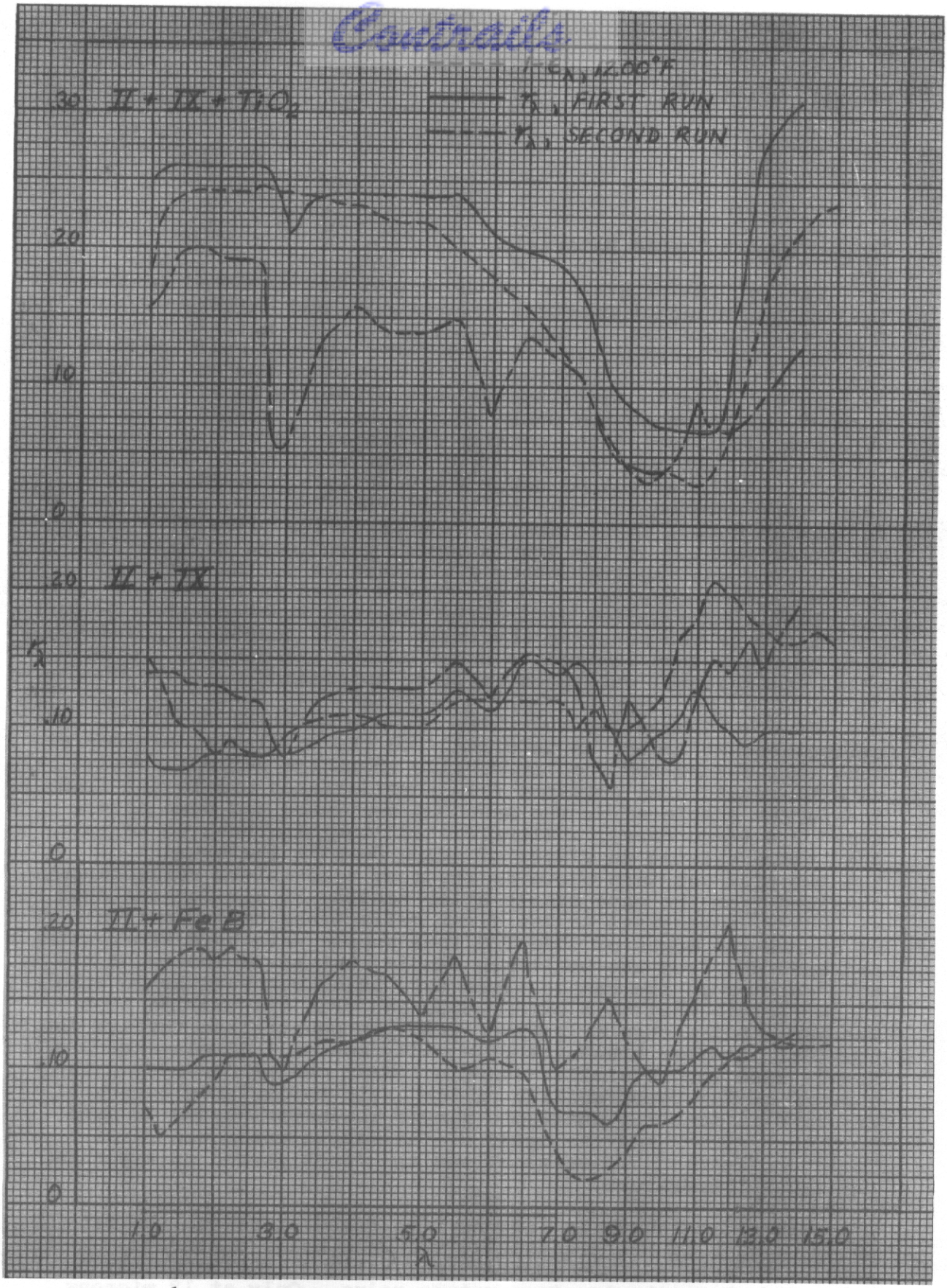

Fig. 6: Spectral Reflectance of Chance Vought Ceramic Coatings

is this difference large.

Similar results were obtained with CV II + Ferroboron, though with it the high temperature reflectance becomes lower at long wave lengths. For the material CV II + IX plus a coating of flame sprayed TiO_2, higher reflectances were produced by the TiO_2 coating but the effect of temperature on the reflectance is again relatively small, with lower reflectances indicated at the higher temperature.

2.4 The Effect of Temperature on the Optical Constants

There are apparently no clear present appraisals of a predicted effect of temperature on the optical constants of dielectric materials and consequently on the spectral reflectivity that is determined by these constants. In the absence of firm theoretical guides for the consideration of results such as have been presented, even qualitative considerations may be useful and those associated with the model of a classical oscillator are reviewed briefly here. In that view, the optical properties are given as:

$$n^2 - k^2 - 1 = \sum_i \frac{N_i e^2}{m_i} \cdot \frac{\omega_{oi}^2 - \omega^2}{(\omega_{oi}^2 - \omega^2)^2 + \omega^2 g_i} \qquad 2.1$$

$$2nk = \sum_i \frac{N_i e^2}{m_i} \cdot \frac{\omega g_i}{(\omega_{oi}^2 - \omega^2)^2 + \omega^2 g_i} \qquad 2.2$$

The sum is taken over all the resonant frequencies ω_{oi}; for each of which the damping is g_i ; and at which there are N_i oscillators per unit volume, of effective mass m_i.

If this situation is specialized to a small spectral range in the neighborhood of one of the oscillators, far enough from the resonant frequencies of the others so that there is from them no absorptive contribution and so that their effect in the region concerned is specified only by a refractive index n_1, then for this region the prior equations become:

$$n^2 - k^2 - n_1^2 = \frac{N e^2}{m} \cdot \frac{\omega_o^2 - \omega^2}{(\omega_o^2 - \omega^2)^2 + \omega^2 g} \qquad 2.3$$

$$2nk = \frac{N e^2}{m} \cdot \frac{\omega g}{(\omega_o^2 - \omega^2)^2 + \omega^2 g} \qquad 2.4$$

Following Moss[2], the optical constants in the region of the resonant frequency can be approximated fairly by taking

$$\frac{\omega_o^2 - \omega^2}{\omega g} \approx \frac{2(\omega_o - \omega)}{g} \equiv X \quad \text{AND} \quad \frac{Ne^2}{m\omega g} \equiv P \qquad 2.5$$

Equations 2.3 and 2.4 then assume the simpler form

$$n^2 - k^2 - n_1^2 = \frac{pX}{1 + X^2} \qquad 2nk = \frac{p}{1 + X^2} \qquad 2.6$$

The numerical calculation of the optical constants and from them of the normal reflectance

$$r = \frac{(n-1)^2 + k^2}{(n+1)^2 + k^2} \qquad 2.7$$

is still tedious and is not expressible in any algebraic form simple enough for analysis. Further, the expression of arithmetic results is complicated by the need to assign values of the refractive index n_1 and the value of p, so that special cases must be considered. Figure 7 shows the normal reflectance that is predicted for $n_1 = 3$ and $p = 2$, the latter group selected with complete arbitrariness. This produces little change from the reflectance of 0.25 associated with the refractive index $n_1 = 3$; a local reflectance maximum occurs on the low frequency side of resonance and the variation in reflectance is almost symmetrical about the resonance point.

The influence of an increase in temperature is postulated to be a broadening of the band, evident as an increase in "g" together with a possible small effect of thermal expansion, which would decrease N slightly. It is expected that band broadening might be the major effect, so that here an increase in temperature is visualized to increase the damping, g, and to thus decrease quantity p. Figure 7 contains results for various values of p, assumed to differ because of differences in band width. Because the band width enters also into the value of X, which is the abscissa of Figure 7, that abscissa has been normalized in measures of the damping g that is associated with $p = 4$. In addition to the reflectance calculated from Equation 2.6, the absorption coefficient is shown also to illustrate the increase in band width associated with smaller values of p.

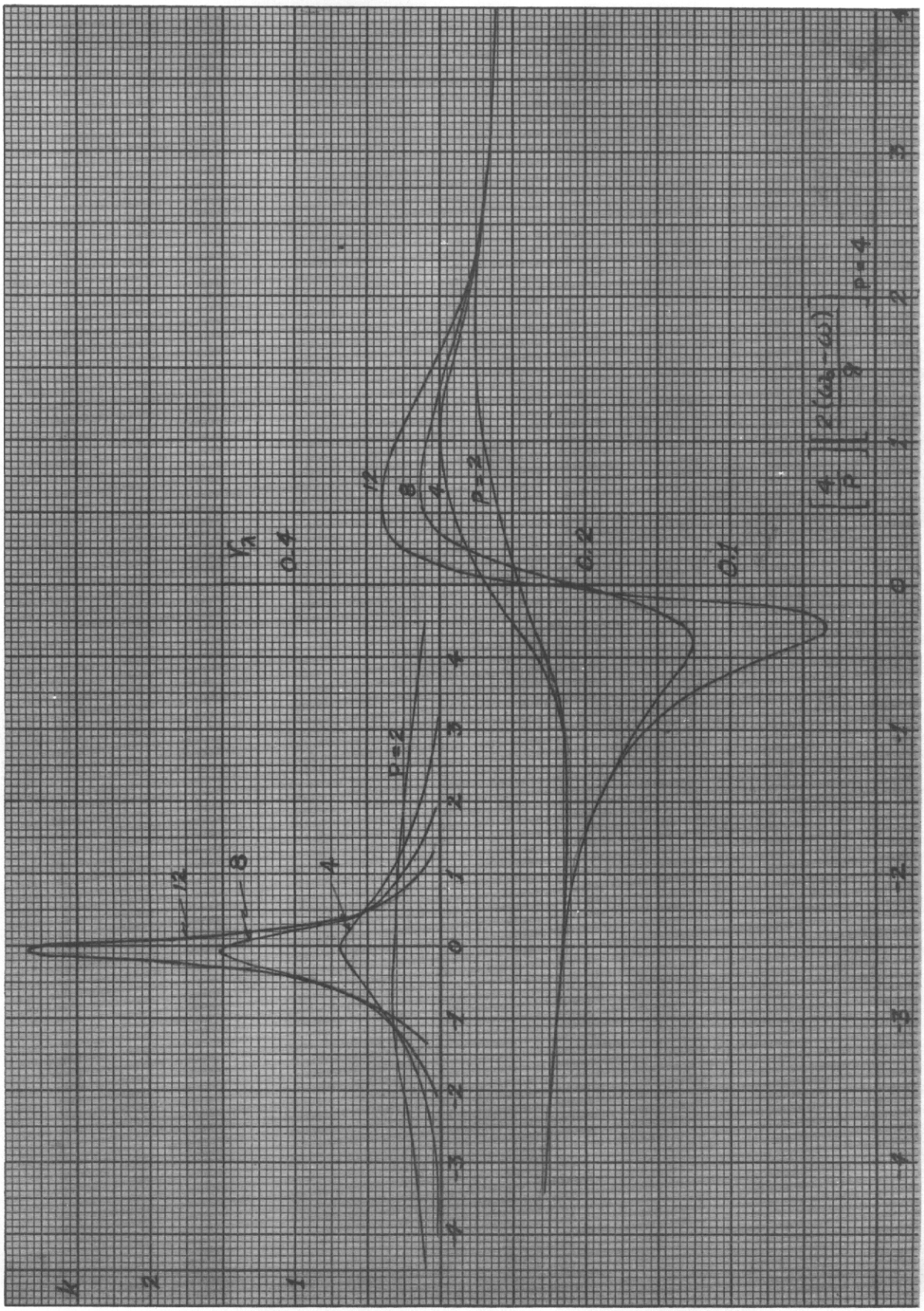

Fig. 7: Effect of Band Broadening on Spectral Reflectance

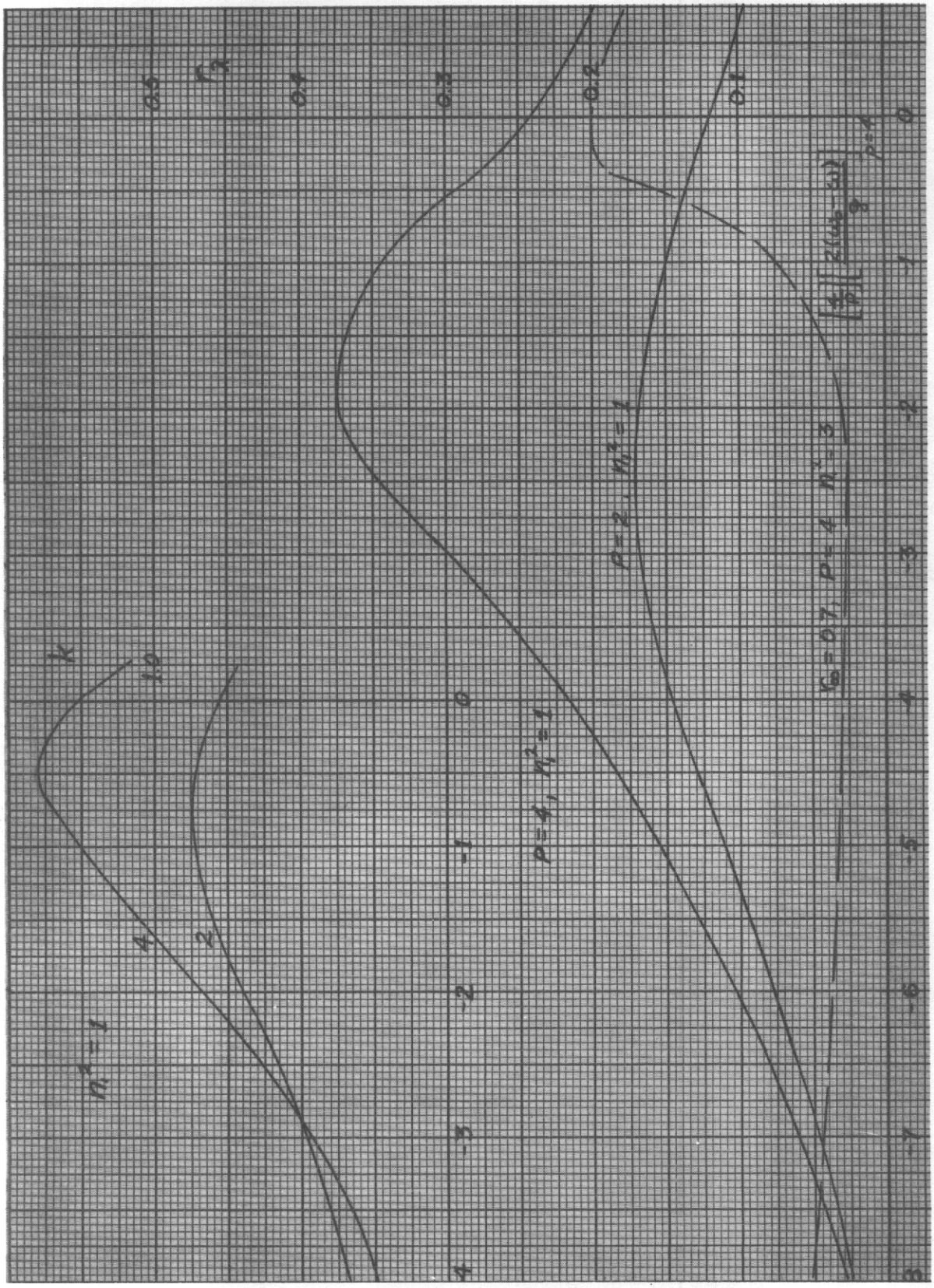

Fig. 8: Effect of Band Broadening on Spectral Reflectance

Since the index of refraction, n_1, is taken as a fairly high value, the qualitative picture shown on Figure 7 must be associated with a fairly narrow spectral region and the local effects associated with this oscillator. With a narrow band width there is a pronounced variation in reflectance, with a minimum on the high frequency, short wave length, side of resonance. As the band width increases, the variation is smoothed out and the local variability of the reflectance is diminished. But in the present results such a behavior for the reflectance is shown only for oxidized nickel in the region of 10 microns, while all the other materials show either ill-defined or opposite effects.

Figure 8 shows additional results obtained from Equation 2.6 and 2.7, primarily for $n_1 = 1$, so that the single oscillator is construed now to be the controlling influence on the index of refraction over broad spectral regions, as in the sense of the optical properties that are determined by lattice vibrations at reststrahlen frequencies. The reflectance maximum now occurs on the high frequency side of resonance and a broadening of the band produces the spectral reduction in the maximum reflectance. At high frequencies the reflectances approach each other gradually. This behavior is suggestive of that of much of the experimental data, for which at short wave lengths the low temperature reflectance exceeds in increasing amount the high temperature value as the wave length increases. The reduced reflectance in the region of the reflectance maximum is indicated experimentally by the majority of the results, though Inconel and HS25 are exceptions.

The foregoing analysis of course assumes a homogeneous film, which is not the nature of the oxides and coatings for which the experimental results have been obtained. In fact, the non-homogeneity that must exist may lead to different behavior than that indicated above because of the effect of inter-reflections within the material. This effect will increase the reflectance when k is small, for then the radiation can penetrate the material and so be subject to inter-reflection, while when k is large this cannot take place and the reflection will be that associated with a homogeneous film. This behavior can then diminish the kind of variation of reflectance shown on Figures 6 and 7 and conceivably could invert it.

III

TEMPERATURE EFFECTS ON THE REFLECTANCE OF METALS

3.1 Introduction

A classical prescription for the prediction of the total normal emissivity of metals is the equation which is obtained from the Hagen-Rubens relation for the spectral emissivity. The total normal emissivity so specified is

$$\epsilon = 0.576\sqrt{\rho T} \qquad \rho \text{ IN OHM-CM}, \quad T \text{ IN } ^\circ K \qquad 3.1$$

Other forms of this kind of result have been obtained by retaining additional terms from the expansion from which the spectral result originates. Similar expressions for the hemispherical total emissivity have been obtained by first integrating the spectral value over the 2π solid angle into which the emission occurs. Jakob[3] summarizes such results which are largely those of Schmidt and Eckert[4]. Abbott et al[5], retain additional terms in the expansion to express Equation 3.1 as

$$\epsilon = 0.578\sqrt{\rho T} - 0.179\,\rho T + 0.44(\rho T)^{3/2} \qquad 3.1a$$

and they demonstrate that this predicts well the total emissivity of platinum which they measured at temperatures as high as 1500°C.

Enough is known about the spectral emissivity and optical properties of those metals, for which Equation 3.1 appears to apply, to establish the inapplicability of the simple Drude theory, of which the Hagen-Rubens relation is the asymptotic form for long wave lengths. The correspondence that is achieved in the case of the total emittance appears therefore to be a kind of coincidence and the present purpose is a review of the spectral properties of the transition metals nickel and platinum, together with theories which support their properties particularly at elevated temperatures, in an effort to establish the reason for the apparent suitability of Equation 3.1 for the prediction of the total emissivity.

3.2 Spectral Emissivity and Optical Constants

Electromagnetic theory specifies the normal emissivity in terms of the complex dielectric constant, $n + ik$. In the nomenclature of Pepperhoff[5] this emissivity is

$$\epsilon = \frac{2\sqrt{2\sqrt{\alpha^2+\beta^2} + \alpha}}{\sqrt{\alpha^2+\beta^2} + 1 + \sqrt{2\sqrt{\alpha^2+\beta^2} + \alpha}} \qquad 3.2$$

where $\alpha = n^2 - k^2$ $\qquad \beta = 2nk$

The dispersion can be evaluated from the classical/free electron theory of Drude, which gives

$$n^2 - k^2 = 1 - \left(\frac{\lambda}{\lambda_1}\right)^2 \frac{1}{1 + \left(\frac{\lambda}{\lambda_2}\right)^2} \qquad 3.3$$

$$2nk = \left(\frac{\lambda}{\lambda_2}\right)\left(\frac{\lambda}{\lambda_1}\right)^2 \frac{1}{1 + \left(\frac{\lambda}{\lambda_2}\right)^2} \qquad 3.4$$

where $\lambda_1 = \sqrt{\frac{\pi m c^2}{N e^2}}$ a wave length close to the location of the minimum of the reflectivity

$\lambda_2 = \frac{2\sigma_0}{c}\lambda_1^2$ the "relaxation" wave length,

associated with the DC conductivity $\sigma_0 = \frac{Ne^2}{m}\tau$, ($\tau$ is the relaxation time). For $\lambda > 10\lambda_2$, approximately, Equations 3.2, 3.3, 3.4 give the asymptotic form

$$\epsilon = 2\sqrt{\frac{\nu}{\sigma_0}} = 2\sqrt{\frac{c}{\lambda\sigma_0}} \qquad 3.5$$

This is the Hagen-Rubens form for the spectral emissivity. In practical units Equation 3.5 becomes

$$\epsilon = 0.365\sqrt{\frac{\rho}{\lambda}} \qquad \rho \text{ IN OHM-CM}, \ \lambda \text{ IN CM} \qquad 3.5a$$

A useful interpretation proceeds from Equation 3.3 and 3.4 when $\lambda > \lambda_1$, so that $(k^2 - n^2) \gg 1$. Then if $(k^2 - n^2)$ and $2nk$ are represented on an Argand diagram there is obtained a straight line of slope $1/\lambda_2$. Locations of particular wave lengths along this line depend, of course, upon the actual values of both λ_1, and λ_2 and for $\lambda \to \infty$, the line terminates at an ordinate $2nk/\lambda = \sigma_0/c$

Equations 3.3 and 3.4 represent the optical constants of metals in regions in which internal photoelectric absorption is small enough to be negligible. Givens[7] shows this correspondence for a number of metals, though a fit of the experimental results by Equation 3.3 and 3.4 demands, in particular, the assumption of a conductivity, σ_0, that is considerably below the D. C. value. This difference is in part due to the surface stress in the specimens from which were determined the experimental values, but even under the best conditions the conductivity required by the theory is of the order of two thirds of the D. C. value and in some cases this factor is one tenth.

In transition metals, such as nickel and platinum, the frequency limit on internal photoelectric absorption decreases, and the effect is important at wave lengths as great as 5 to 10 microns. Most of the values of the optical constants of these metals are available only for shorter wave lengths, making impossible a logical fit on the basis of Equations 3.3 and 3.4. For nickel, however, Beattie and Conn[8] obtained optical constants at wave lengths as high as 14 microns both at 20°C and 270°C and they plotted these results on the Argand diagram to establish a line representing the Drude theory in terms of the presumed asymptotic behavior of the optical constants at long wave length. Figure 9 shows these results for both electropolished and buffed nickel and for the latter there is indicated the associated Drude line. It is, however, not clear from this work how the wave length scale was established on the Drude curve, that is, how λ_1, was chosen, though the chosen values are realistic in terms of (N/m)*.

*(The ambiguity does not occur in the case when at least one experimental value falls on the line, for this establishes one wave length on it and this was, in fact, the situation in the only case in which Beattie specified directly the way in which the wave length scale was established.)

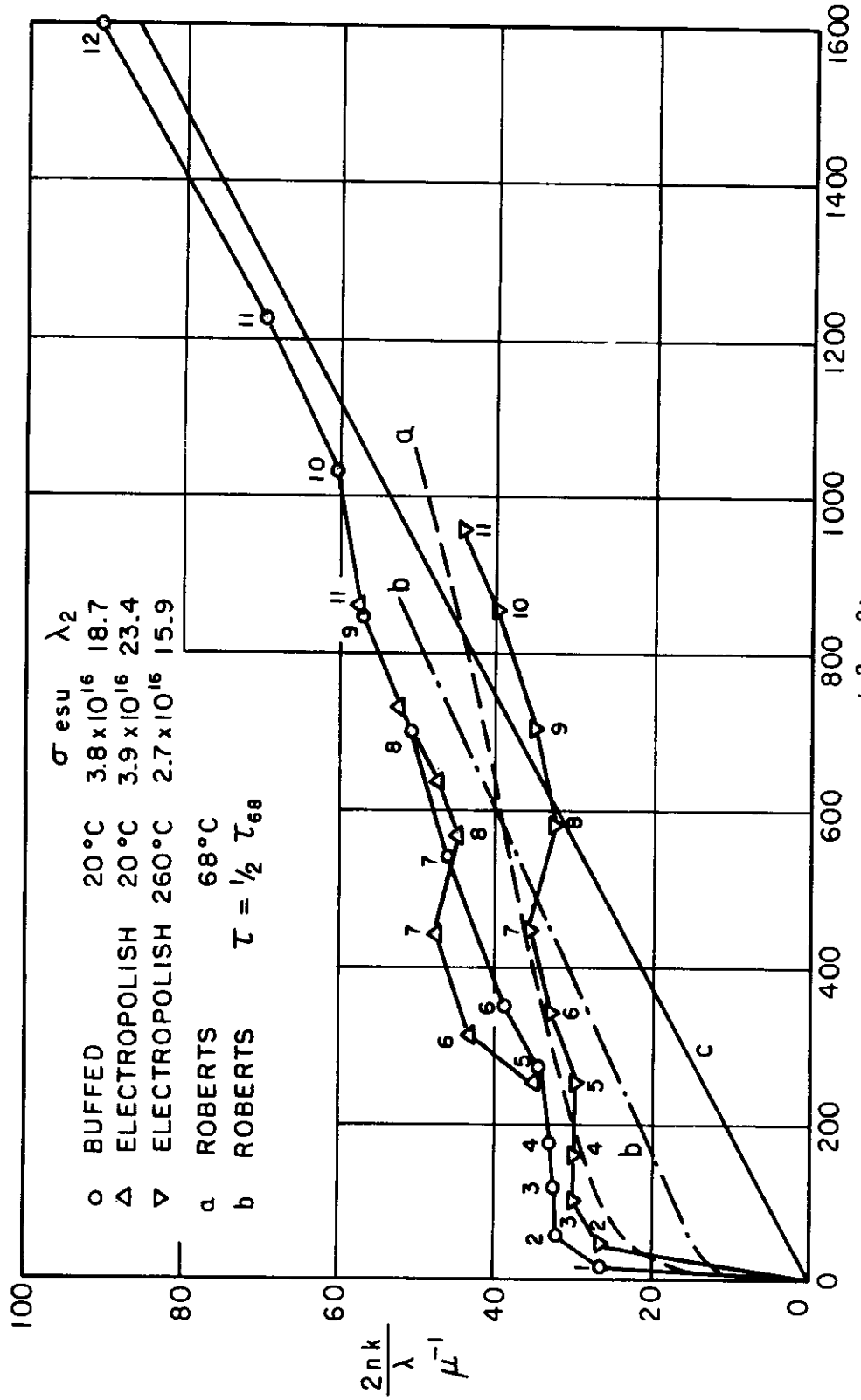

Fig. 9: Optical Constants of Nickel (8)
The points are those of Beattie. Line "c" is the Drude line assumed for buffed nickel.

With wave lengths known both on the Drude line and for the experimental data, Beattie connected corresponding points by vectors, the components of which, $2nk/\lambda$ and $(k^2 - n^2)$, represented the contribution of the anomalous absorption. He observed that this contribution was essentially independent of temperature insofar as could be deduced from his results at 20°C and 250°C. If this assumption is maintained for all temperatures then the contribution of the anomalous absorption, known as a function of the wave length, can be added to that of the Drude theory as evaluated implicitly for various temperatures by selection of appropriate values of λ_2 .

In another point of view, Roberts[9] has shown that by using the Drude theory for a double set of charge carriers (which is its original form), the optical constants for nickel, platinum, and iron could be specified, and on this basis the conductivity that is needed in the theory is much closer to the DC value than that which is required in the usual application of that theory. The optical constants are then given in the terms:

$$n^2 - k^2 + K_\infty = \frac{\lambda^2}{2\pi c}\left(\frac{\sigma_a \lambda_{2a}}{\lambda_{2a}^2 + \lambda^2} + \frac{\sigma_b \lambda_{2b}}{\lambda_{2b}^2 + \lambda^2}\right) \qquad 3.6$$

$$\frac{2nk}{\lambda} - \frac{\sigma_\infty}{2\pi c} \qquad \frac{\lambda^2}{2\pi c}\left(\frac{\sigma_a}{\lambda_{2a}^2 + \lambda^2} \qquad \frac{\sigma_b}{\lambda_{2b}^2 + \lambda^2}\right) \qquad 3.7$$

with the following values of conductivity and relaxation wave length for room temperature.

Table I

	λ_{2a} Micron	λ_{2b} Micron	$\sigma_1 \times 10^{-6}$ ohm Meter	$\sigma_2 \times 10^{-6}$ ohm Meter
Pt	1.27	205	1.03	8.22
Ni	.70	44	.45	7.90
Fe	.39	75	.24	9.52

Optical constants found from Equations 3.6 and 3.7 and the values given in the Table are shown on Figure 9 and these correspond well with the experimental values for electropolished nickel at wave lengths below 7 microns.

To obtain a prediction for higher temperatures an estimate must be made regarding the effect of temperature on the relaxation wave lengths λ_{2a} and λ_{2b}. It might be assumed that they decrease equally and Figure 9 contains the optical constants that are indicated by a reduction of one half in both of the wave lengths. The relative effect that is obtained in this way is at short wave lengths opposite to the trend found experimentally by Beattie and there are evident no alternative assumptions which would improve the nature of the temperature dependence of the optical constants as they are prescribed by Roberts theory.

Roberts' equations, with the values given in Table I, are shown by him to fit available optical properties for wave lengths up to 4 microns, and they will do so fairly for constants available up to 5 microns. Spectral emissivities calculated from these constants do not, except for magnitude, correspond well with measured values for $\lambda > 1$ micron, so that there is some question as to the validity of the constants at these wave lengths. The constants available for platinum do not, moreover, extend to wave lengths large enough to enable an appraisal such as presented for nickel by Beattie. In consequence, there turns out to be almost no support from data on optical constants for the spectral emissivities that have been determined for platinum.

3.3 Spectral Normal Emissivity of Nickel

Figure 10 shows the spectral normal emissivity that is calculated from Equation 3.2 for buffed nickel from the optical constants that were obtained by Beattie and which are shown in Figure 9, and beyond 10 microns from the Drude theory associated with those results. At very long wave lengths there is shown the magnitude of Equation 3.5 to which the Drude result becomes asymptotic. For comparison, there is also shown the position of Equation 3.5, the Hagen-Rubens law, when the D. C. conductivity is used therein.

Values of the emissivity for higher temperatures are shown in terms of the prediction from Beattie's results for smaller values of λ_2, though to make these results specific a relation between λ_2 and the temperature must still be chosen. The position of Equation 3.5 is indicated for conductivities which are one quarter of the room temperature values, and as the value of λ_2 decreases, the Drude contribution approaches the linear form of Equation 3.5 and the anomalous contribution is proportionately less, so that the form of the spectral emissivity curve becomes increasingly like that of Equation 3.5.

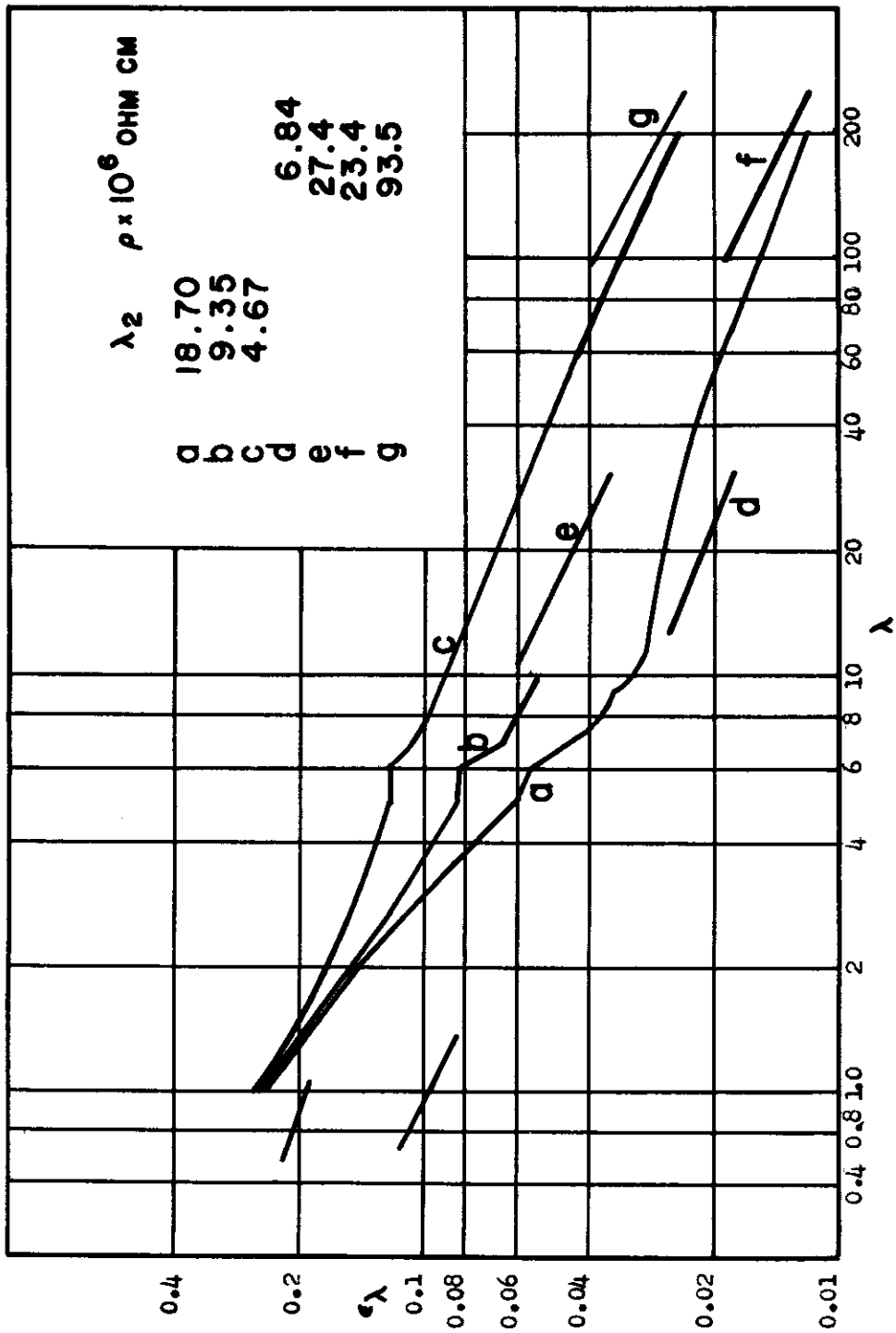

Fig. 10: Predicted Values of the Spectral Emissivity of Nickel.
Curves a, b, and c are derived from the results of Beattie.
Curves d, e, f, g, are Eq. 3.5 for the indicated resistivities.

Values of the spectral emissivity were calculated also from Roberts' theory with the additional postulate that both of the relaxation wave lengths diminish equally. Figure 11 shows the results, for reductions in relaxation wave length comparable to those which yielded from Beattie's presentation the results shown on Figure 10. For room temperature the emissivity that is predicted is comparable in form though lower than that given on Figure 10, an expected result because of the lower absorption of Roberts' prediction, which is comparable to that of electropolished nickel. Reduced values of λ_2 produced a small effect, though the emissivity near 10 microns increases substantially as λ_2 is reduced. Rationalization of these effects is, however, difficult because of the complex way in which the optical constants are involved in Equation 3.2.

Figure 12 shows some experimental values for the spectral emissivity of nickel at room temperature, obtained as reflectance in a cavity (Gier-Dunkle) reflectometer, and in an integrating sphere. These values are higher than those predicted from the optical constants of Figure 9 (Curve a) and the excess is probably due to a greater surface stress in the polished sample from which the reflectance values were obtained. At long wavelengths the emissivity is low and the poor accuracy of the results is evident in their scatter.

The only results available at higher temperature appear to be those of Hurst[10], obtained as emissivities in a vacuum for wave lengths between 1 and 6 microns. These are shown on Figure 4, and compared to the absorptivities for low temperature, their relative magnitude is remarkably like the similar relation between the predictions for low temperature and for one half the relaxation wave length typical of the low temperature. Curve "k", which represents Equation 3.5 evaluated with the D. C. conductivity corresponding to 2290°R, shows that this predicts the magnitude of Hurst's results and is in fact considerably better than the similar correspondence at low temperature between experiment and Equation 3.5.

3.4 Spectral Normal Emissivity of Platinum

Results are available for the optical constants of platinum only at room temperature and for short wave lengths, and these can be represented by Roberts' equation evaluated with the magnitudes contained in Table I. When the optical constants so obtained are used in Equation 3.2 for the evaluation of the emissivity, the predicted values are completely at variance with experimental results. In addition, when predictions for reduced relaxation times are made, as they were for nickel to give

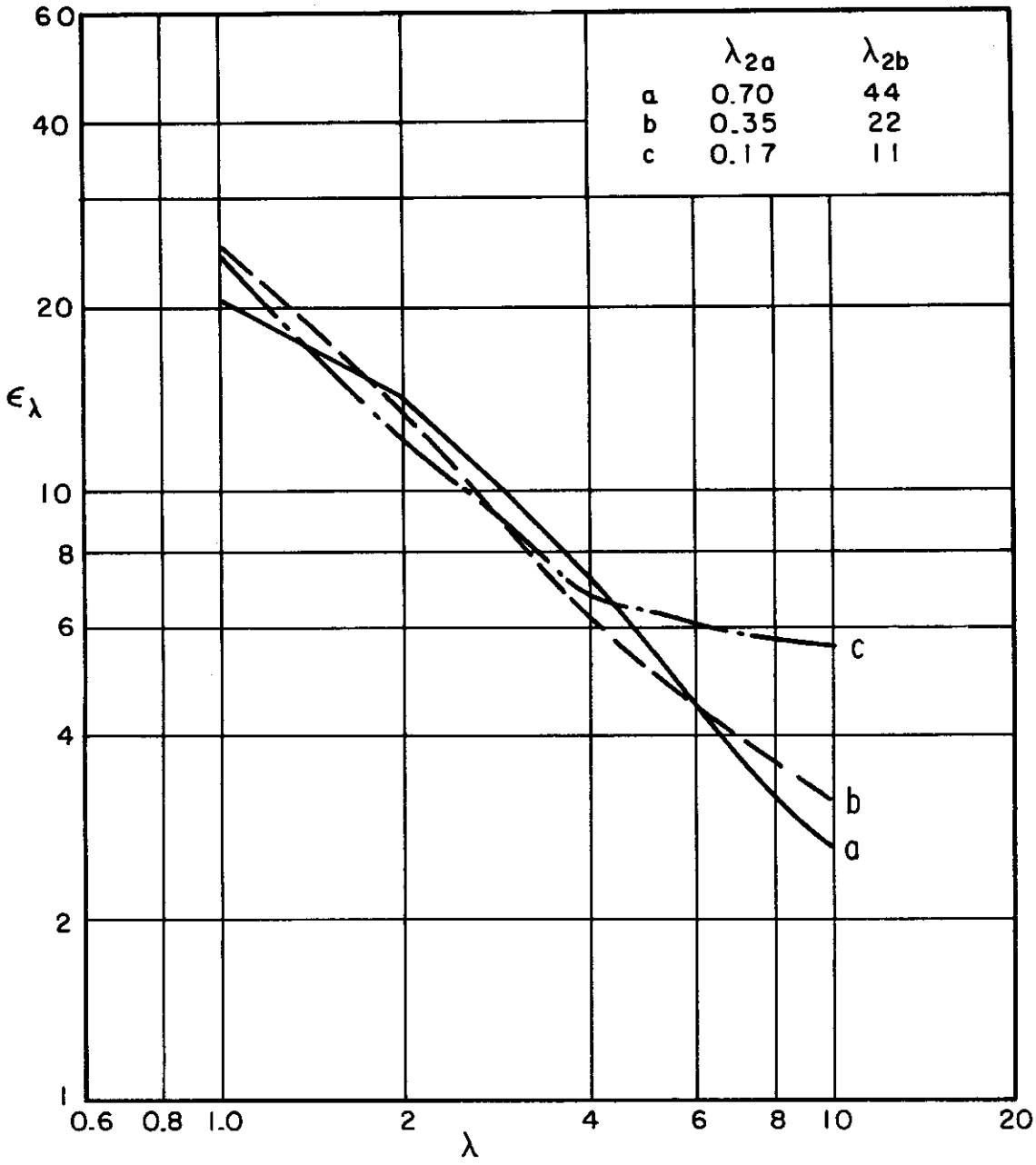

Fig. 11: Spectral Emissivity of Nickel from Roberts Theory.

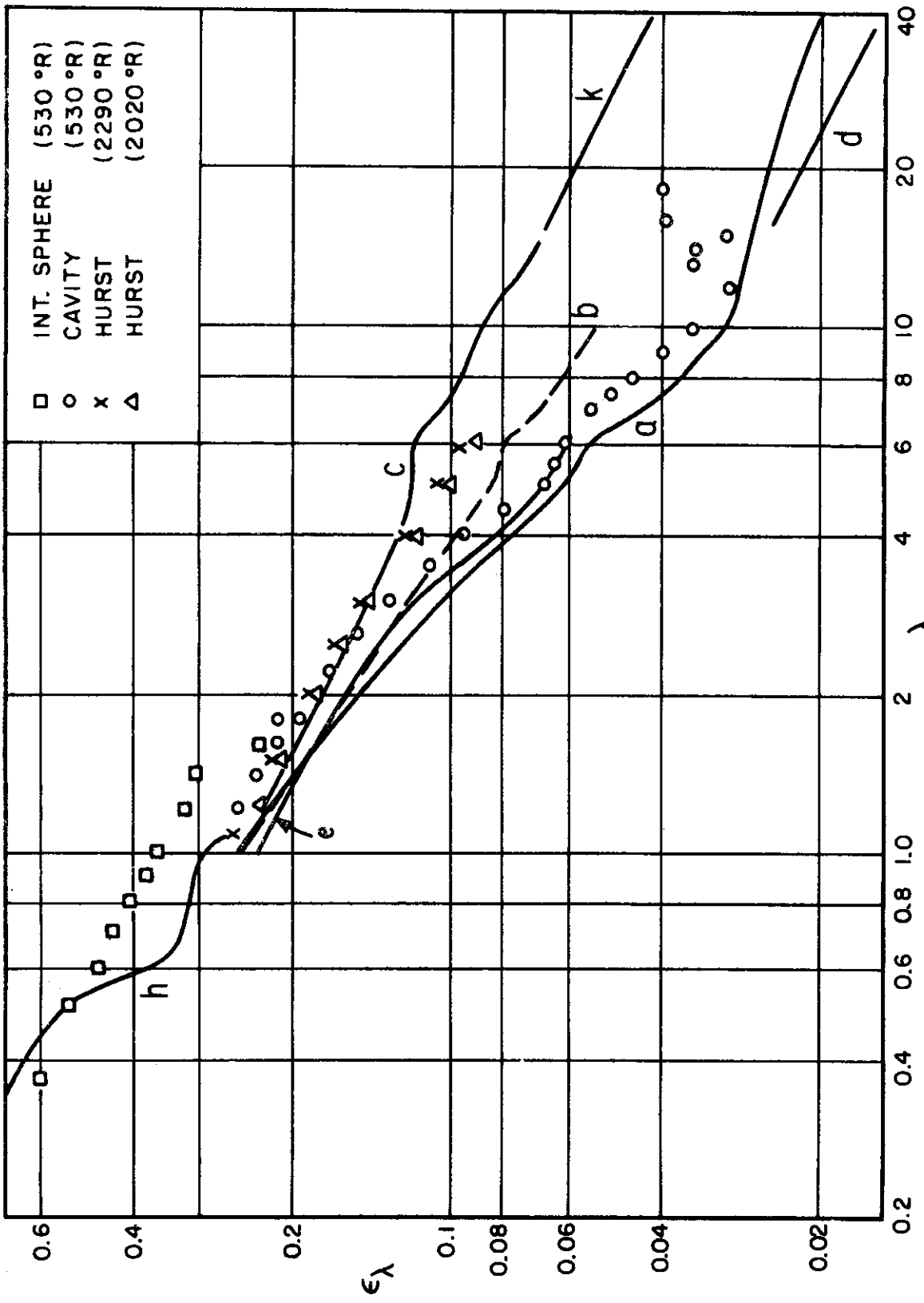

Fig. 12: Experimental Spectral Emissivity of Nickel. Curves a, b, c, d, are from Figure 10. Curve e, Hagen Rubens experimental, from Hurst[10]. Curve h, Pepperhoff (6); curve k, Eq. 3.5 for resistivity at 2000°R.

the results shown on Figure 11, the spectral emissivity is found to increase substantially at short wave lengths and insignificantly at long wave lengths. It is inferred that the presently known optical constants may be of insufficient accuracy, and they are certainly not known at sufficiently large wave lengths, to permit an acceptable prediction of the spectral emissivity. The further consideration of the experimental values of the emissivity therefore lacks the guidance of any theoretical prediction.

Figure 13 contains values of the emissivity inferred from experimental values of the reflectivity measured at room temperature. These reflectances are high and the consequent experimental scatter is severe, more so than in the case of nickel. The two sets of data shown are at some variance, a difference perhaps attributable to cleaning procedures, or to changes in the surface, as the lower of the reflectances obtained at low temperature were secured after the sample had been heated to 1900°R in an emittance determination. The higher of the two reflectances agree reasonably with the reflectance curve given by Pepperhoff[6].

Results at higher temperature were obtained both as emittance and as reflectance, with generally satisfactory agreement between the two results. With respect to those for room temperature, there is revealed the same trend as was apparent for nickel, which entails a substantial increase in emittance at long wave lengths and an inappreciable effect for wave lengths between 1 and 3 microns.

Positions are shown for the lines describing Equation 3.5, the Hagen-Rubens law, evaluated with the D. C. resistivity corresponding to the temperatures involved. Particularly at the higher temperatures this represents the results quite well.

3.5 Total Normal Emissivity

Total normal emissivities can be obtained by integration of the spectral values and these total values are of interest both for appraising how well such total values agree with those that have been measured directly and also for examining further the apparent worth of Equation 3.1 for the prediction of these values when that equation is evaluated on the basis of the D. C. conductivity. The total values obtained from spectral values are, however, subject to varying degrees of uncertainty, depending on the proportion of the black body emissive power that is contained in spectral regions in which the spectral emissivity is not actually known. Table II contains such fractions for various temperatures.

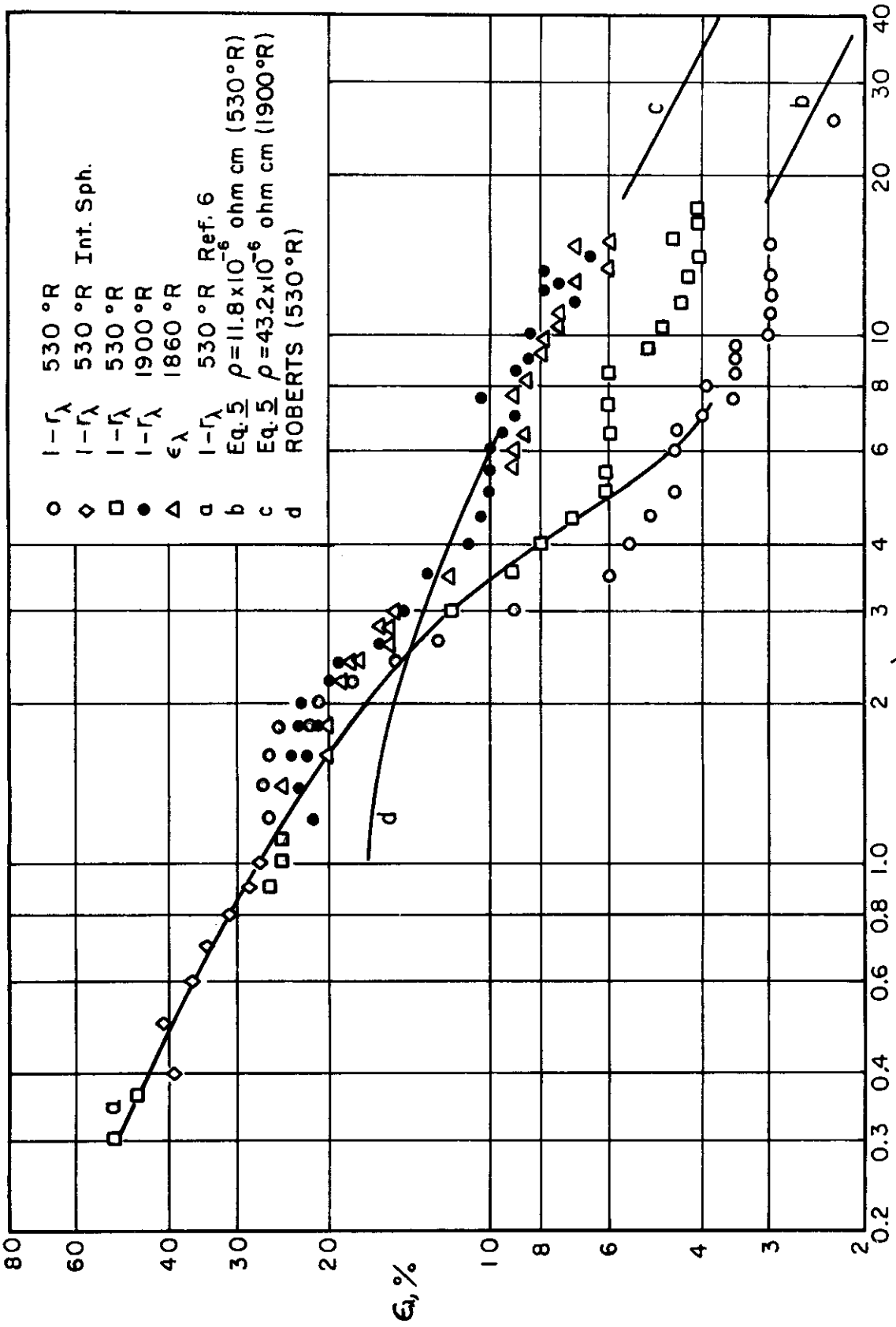

Fig. 13: Experimental Spectral Emissivity of Platinum.

Table II

Temp. °F range microns	500	1000	2000	3000	4000	solar
below 0.3						.014
below 0.5				.00	.00	.24
below 1.0	.00	.00	.00	.02	.10	.71
above 10	0.78	0.30	.07	.03	.01	.00
above 20	0.30	0.07	.03	.00	.00	.00

Clearly, the availability of spectral values in the range from 1 to 20 microns provides for reasonable predictions for temperatures from 1000 to 4000°R, while for 500°F there is considerable uncertainty which must be resolved by some appropriate estimate of the emissivity for longer wave lengths.

Total normal emissivities for nickel are shown on Figure 14 and that figure contains a curve which represents experimental values of the total normal emissivity, the curve being that given by Goldsmith, et. al.(10). A point is shown for 2000°R, as obtained from the spectral emissivity as given by Hurst, together with a slight extrapolation, up to 10 microns, based on the trend revealed by the predicted emissivity. This point is 8% below the curve representing the experimental values. Another point indicates the prediction based on the experimental data for room temperature, together with the presumption that at longer wave lengths the emissivity would be that given by the prediction made from the Beattie results. This point coincides with the experimental curve.

Another curve in Figure 14 indicates the prediction made from Equation 3.1 when the D. C. value of the conductivity is used for the evaluation. The departure from experimental values is not too great between 500°R and 2000°F and this kind of agreement was already indicated on Figure 4 where, particularly at the higher temperature, Equation 3.5 provides a fair approximation to measured spectral values. That coincidence is not quite as good at 500°R, but there a preponderant contribution to the total emissivity is made at longer wave lengths. There are no data in this region, and the relative positions of Equation 3.5 and the Beattie result indicates that a lower emissivity will be obtained from Equation 3.5, as is shown on the Figure.

Finally, there are shown on Figure 14 further points not derived from data but from the results obtained from Beattie, interpreted in a special way. Beattie's results for temperatures of 970°R and 530°R indicated values of λ_2 in the ratio

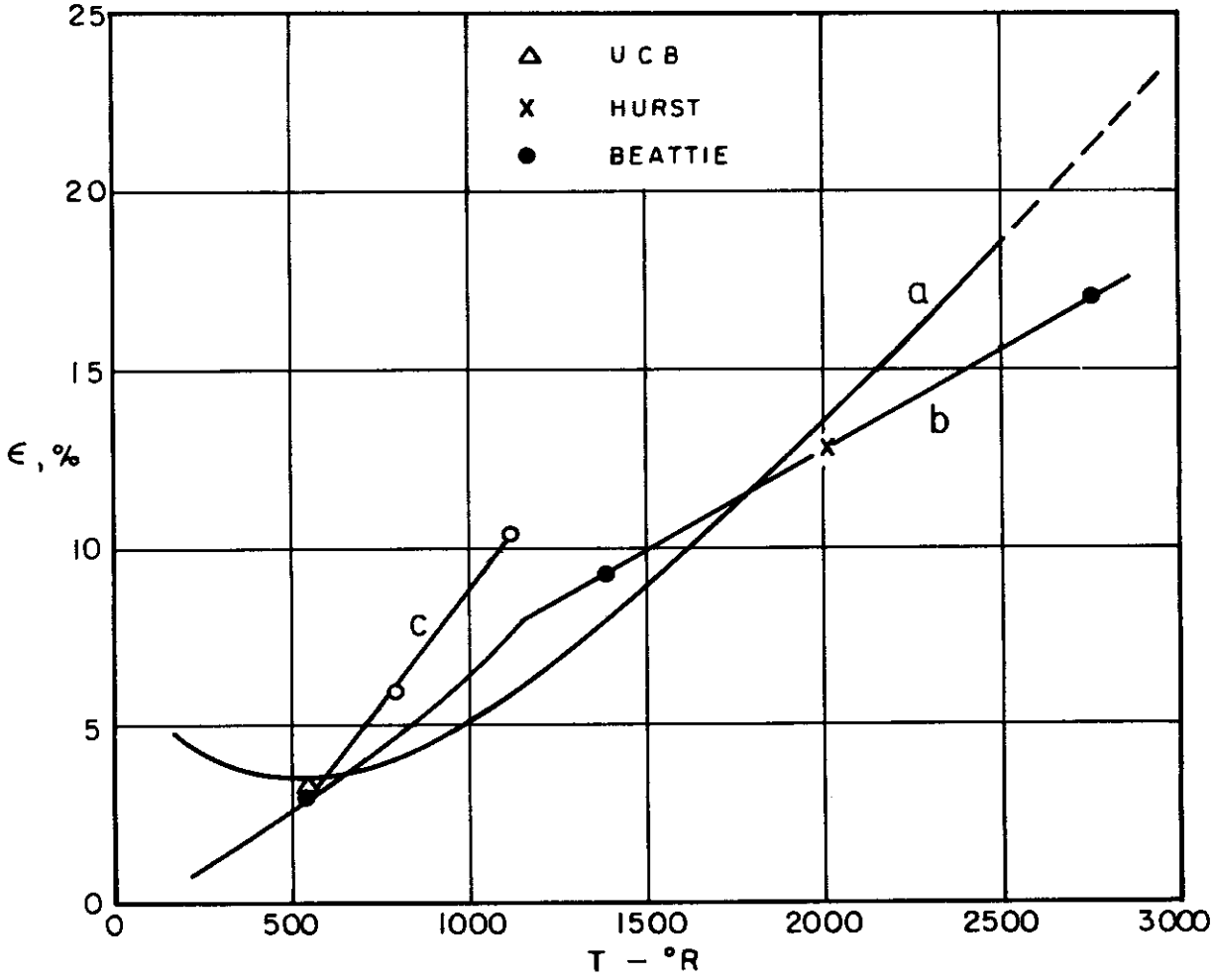

Fig. 14: Total Normal Emissivity of Nickel.
Curve a, from ref. 11; curve b, Eq. 3.1 with D. C. resistivity; curve c, Beattie, with relaxation time proportional to actual conductivity.

of roughly 1.40, a ratio much less than that of the D. C. conductivities at these two temperatures. With the value of λ_z taken to depend on temperature in the way that is inferred from Beattie's results, total emissivities can be calculated from the spectral emissivities associated with the two smaller values of λ_z that are shown on Figure 10. These are shown as points on Figure 14 and these values practically coincide with the prediction from Equation 3.1. Curve "c" of Figure 14, shows in contrast the unsatisfactory values of total emissivity that are predicted from the spectral values shown on Figure 10 if the value of λ_z is taken as inversely proportional to the actual D. C. conductivity.

Total normal emissivities for platinum have been measured by Abbott, et. al. for temperatures from 1400°K to 2400°F and a curve representing these results is shown in Figure 15. Since the resistivity of platinum varies linearly with the absolute temperature, Equation 3.1 indicates that a linear relation is expected for the emissivity. This exists and is the basis for the extrapolation of the experimental line to lower temperatures. Lines for Equation 3.1 are shown on the Figure, for D. C. conductivity evaluated from a reference and also from measurements on the emissivity samples made by Abbott. As shown by him, both are close and the latter evaluation practically coincides with the experimental results.

Abbott's results reveal that higher values of the emissivity are obtained after the sample has been maintained at an elevated temperature for a considerable period of time, an effect due to alteration of the surface of the material, ostensibly caused by recrystallization, which may be initiated at temperatures above about 1500°R. After a long period of heating to temperatures as high as 2500°F, increases in emissivity of the order of 10% were found.

The spectral emissivities shown on Figure 13 have been integrated to obtain total emissivities and the results are shown as points on Figure 15. Considerable uncertainty is associated with the points at room temperature which were obtained by assuming for long wave lengths a spectral emissivity variation of the nature indicated by Equation 3.5, matching the measured values in the region of 10 microns, though the value of λ_z is apparently much smaller for platinum than it is for nickel and this improves the accuracy of this assumption. At 2000°R, the total emissivity obtained from the spectral value is reasonably close to the measured total values. At low temperature the integrated value that is obtained from spectral results corresponds best with the extrapolation of the line representing the measured total emissivities.

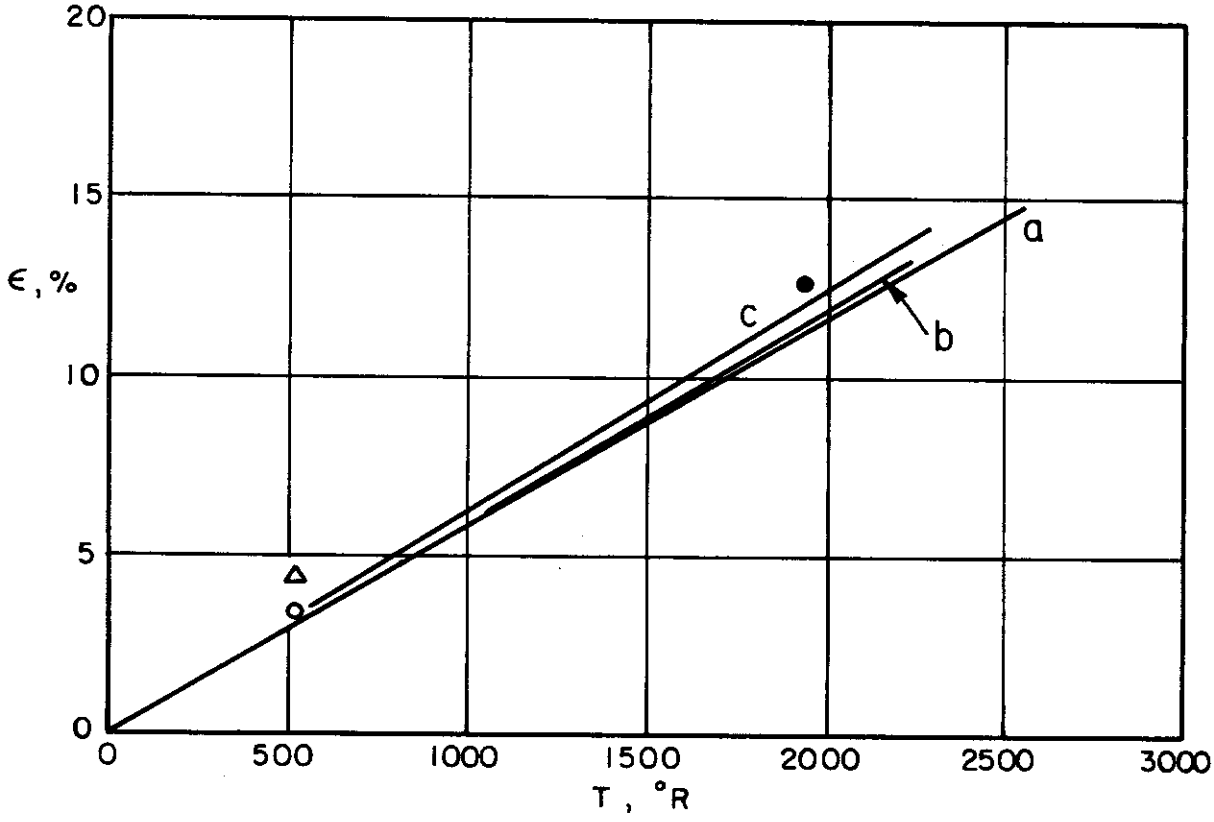

Fig. 15: Total Normal Emissivity of Platinum. Curve a, Abbott, [5] experimental; curve b, Equation 3.1, Abbott resistivity; curve c, same, handbook resistivity. Points correspond to Figure 13.

The applicability of Equation 3.1 in the case of platinum, as it was for nickel, rests on the coincidence that at high temperature it happens to indicate quite well the spectral emissivity for wave lengths from 1 to 15 microns. It does not do so near room temperature, but at that temperature there is a small amount of the total energy in that spectral region and Equation 3.5, from which Equation 3.1 is derived, still gives a fair indication of the magnitude of the spectral emissivity in the region $\lambda > 10$ microns in which the major part of the radiation occurs. Another instance of the applicability of Equation 3.1 is given on Figure 32 for the total emittance of the alloy platinum - 13% rhodium, though in that evaluation there is actually considerable uncertainty regarding the electrical resistivity. While spectral properties are not available to provide reasons for that correspondence, it is expected that the situation relatively is like that for platinum.

3.6 The Effect of Surface Stress

The well known effect of surface stress in altering the optical constants in a way that results in a decrease in the reflectivity of a metal may in itself contribute to a correspondence of the reflectance with the prediction of the Hagen-Rubens law in spectral regions for which the law might not be expected to apply. Such would be the case if the decrease in reflectance was relatively greater at short wave lengths, so that its contribution would produce an effect relatively the same as that of the anomalous absorption that has been previously considered. In this regard there are presented here certain results that were obtained by Russell[12] for the reflectance, at room temperature, of roughened and polished samples of copper and 321 stainless steel which illustrate that one effect of the stress is to make the distribution of the spectral reflectance like that of the Hagen-Rubens law.

Figure 16 presents results for copper and, of the absorptances shown there, only for an electropolished sample was the trend of the absorptance like that expected from the Drude theory. The absorptance of a mechanically polished surface is higher and for wave lengths from 1 to 10 microns this absorptance varies with wave length in the way that is indicated by the Hagen-Rubens law, equation 3.5, though with magnitudes greater than that predicted by that law for the D. C. conductivity at room temperature. This is the behavior that corresponds to the statements that do appear in the literature about the relative suitability of the Hagen-Rubens law for predicting the spectral reflectance of even as good a conductor as copper.

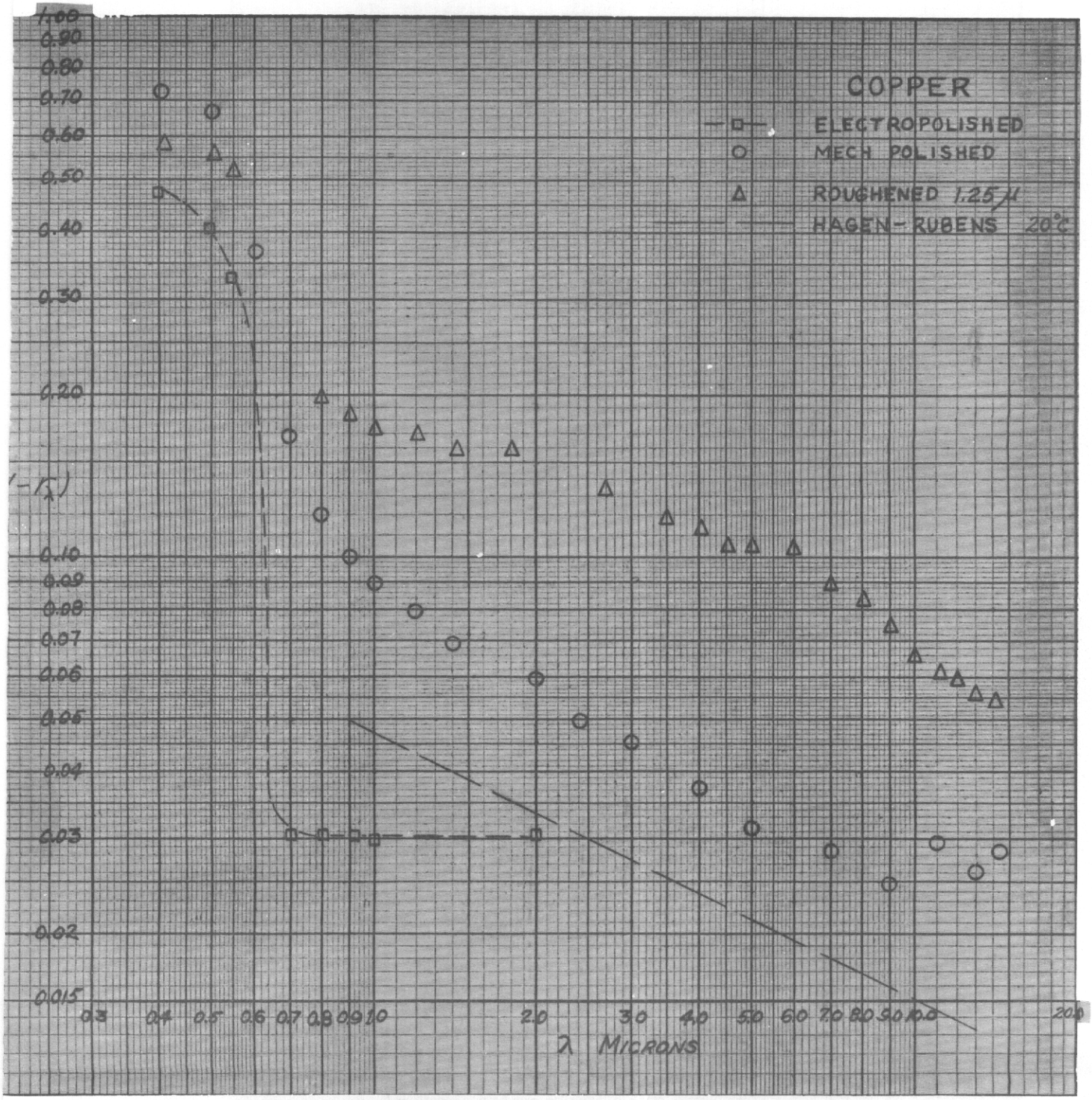

Fig. 16: Spectral Absorptance of Smooth and Roughened Copper

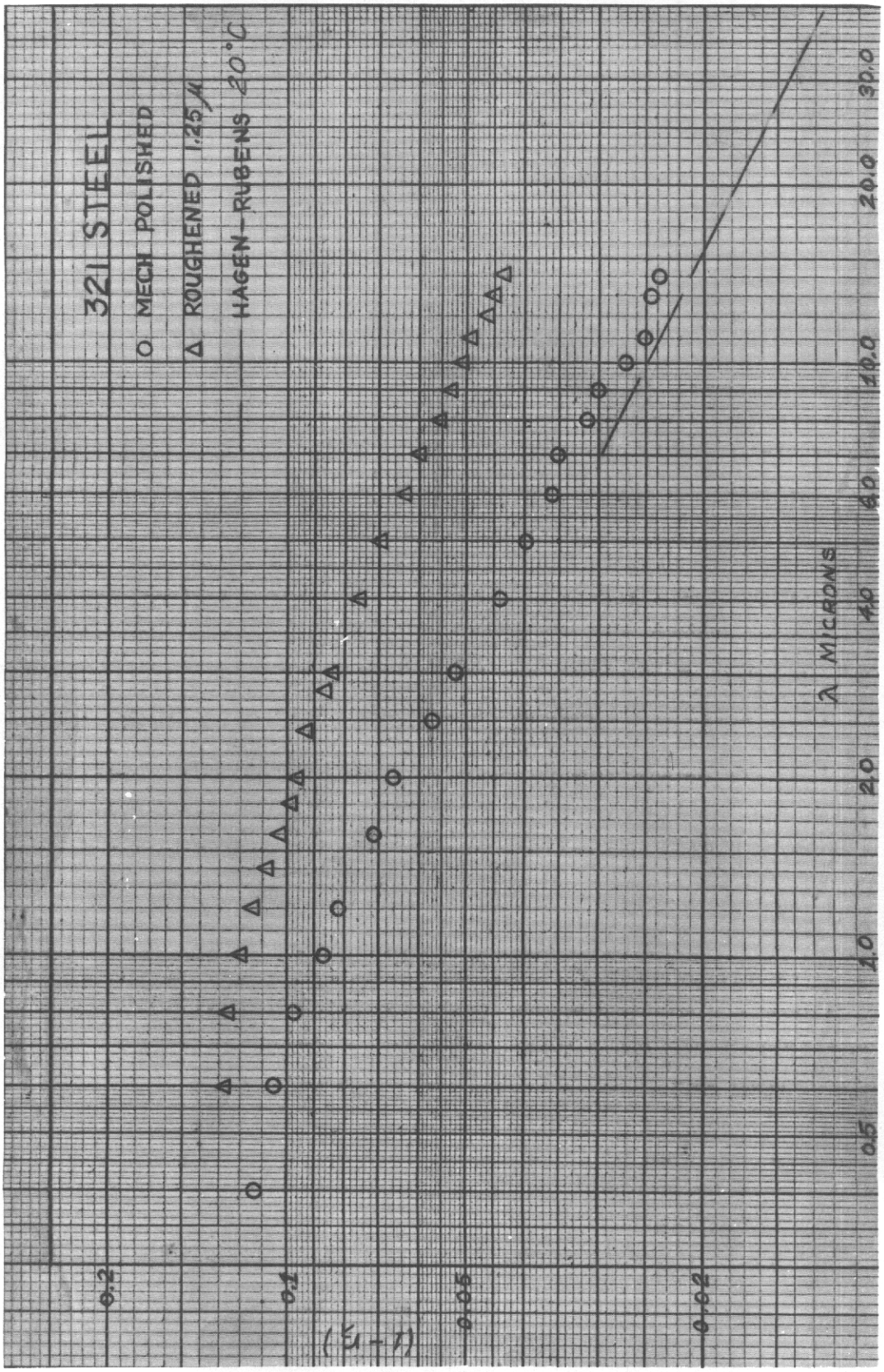

Fig. 17: Spectral Absorptance of Smooth and Roughened 321 Stainless Steel

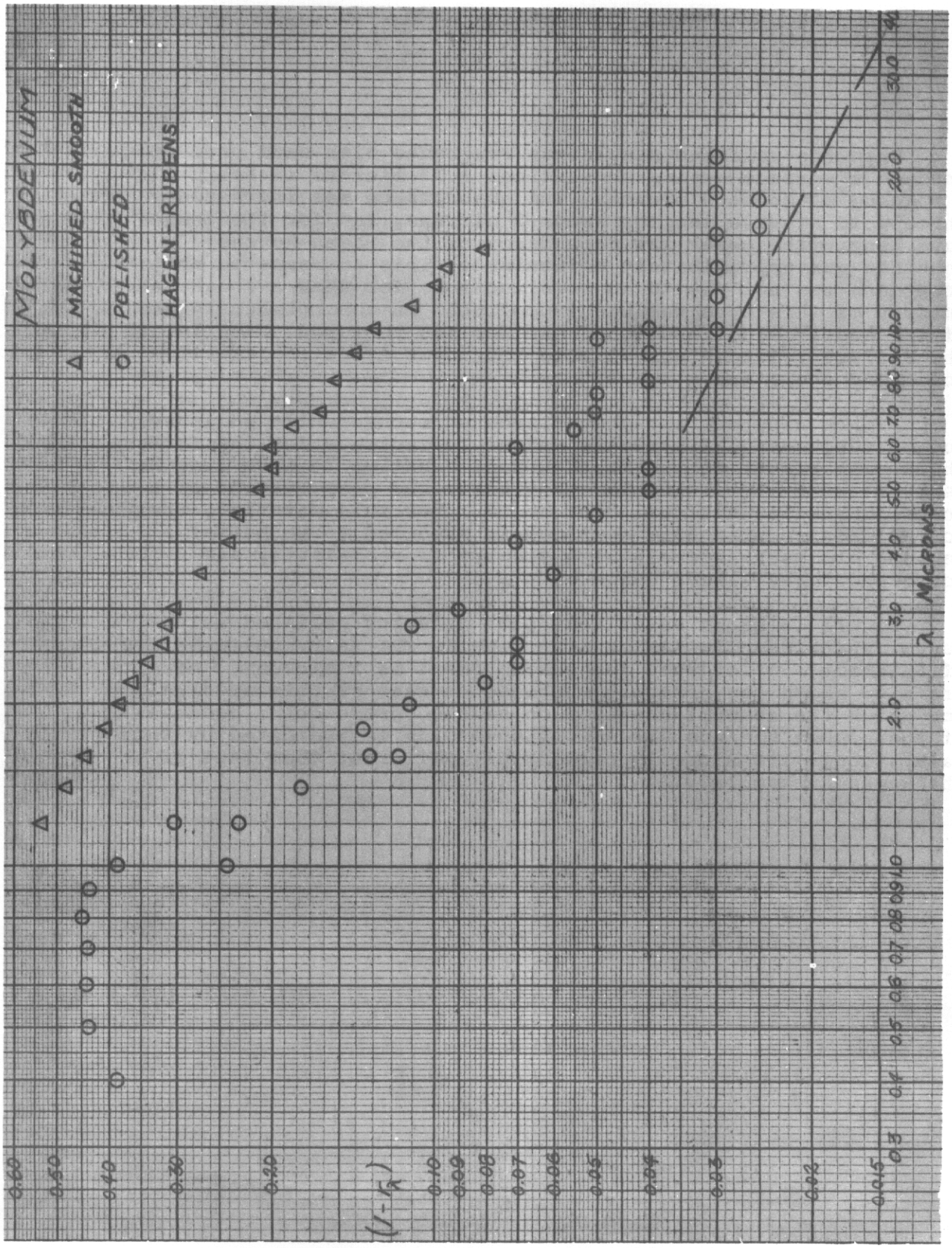

Fig. 18: Spectral Absorptance of Molybdenum

When the polished sample was roughened with sand paper to produce a surface having undulations 1.25 microns in height, at a spacing of about 9 microns, the absorptance was increased three fold at wave lengths above 2 microns, and for the longer wave lengths the power law dependence of the Hagen-Rubens equation was approximately maintained. This increase in absorptance was not due to interreflection, for when a roughened surface of this type was electropolished an absorptance typical of the smooth electropolished surface was restored, even though the surface retained appreciable roughness after the electropolishing operation.

Figure 17 shows the absorptance of mechanically polished and of roughened 321 stainless steel to indicate for the former the applicability of the Hagen-Rubens equation to wave lengths as short as 1 micron and for the latter the preservation of a somewhat similar spectral dependence. For this material, the correspondence with that equation is expected to be better because of its relatively high electrical resistivity and correspondingly larger value of λ_z .

Figure 18 shows relatively poor data for polished molybdenum, which despite its scatter reveals the fair applicability of Equation 3.5 for wave lengths as short as 2 microns. Results are also shown for a smooth machined surface of this material, for which the absorptance is much higher, presumably because of the higher surface stress. A power law is indicated by this data, though its slope is perceptibly different than that of the Hagen-Rubens law.

IV

SYSTEM FOR EMITTANCE DETERMINATION IN AN INERT ATMOSPHERE

4.1 Introduction

The elimination of that aging effect which is due to oxidation of the sample requires a high vacuum or an inert atmosphere to surround the sample for which the radiation properties are to be determined. The system here described achieves this requirement in a unit in which both normal spectral and normal total emittances can be determined in the temperature range from 1500°F to 3000°F. In form, the arrangement that was chosen for this system was that described by the requirement of identical optical paths for observation of the sample and of the reference cavity, together with fixed positions for these two elements. In this respect this system is similar to the intermediate unit which was described before[1] and from which were obtained the results for spectral emittance that appear in this report.

4.2 System and Enclosure

The essential elements, the sample heater and the reference cavity, are located, together with a moveable mirror thru which the line of sight is directed to either of these elements, in a tank which is 16 inches in diameter and 36 inches long. The tank, heater, and cavity are shown on Figure 19 and the axes of all three lie in the horizontal plane. The line of sight for spectral determinations originates from either the sample or from the cavity and by the moveable mirror, positioned externally through a selsyn motor operating against stops, passes through a window in the side of the tank into the conventional collimating system in which the radiation is chopped and focussed on the inlet slits of a Perkin-Elmer Model 98 monochromater. Horizontal slits are located at the focus which exists at the chopper location and these slits, in combination with the vertical monochromator inlet slits, define the area viewed on the sample and on the cavity opening. At the latter location a height, defined by the horizontal slits, of about 3 millimeters has been used at an operating temperature of 1500°F; the width of the viewed area, depending on the monochromator slit opening, is much less.

A system for the measurement of total emittance (not yet installed) consists of a thermopile detector and spherical mirror which focusses energy on the detector from either the

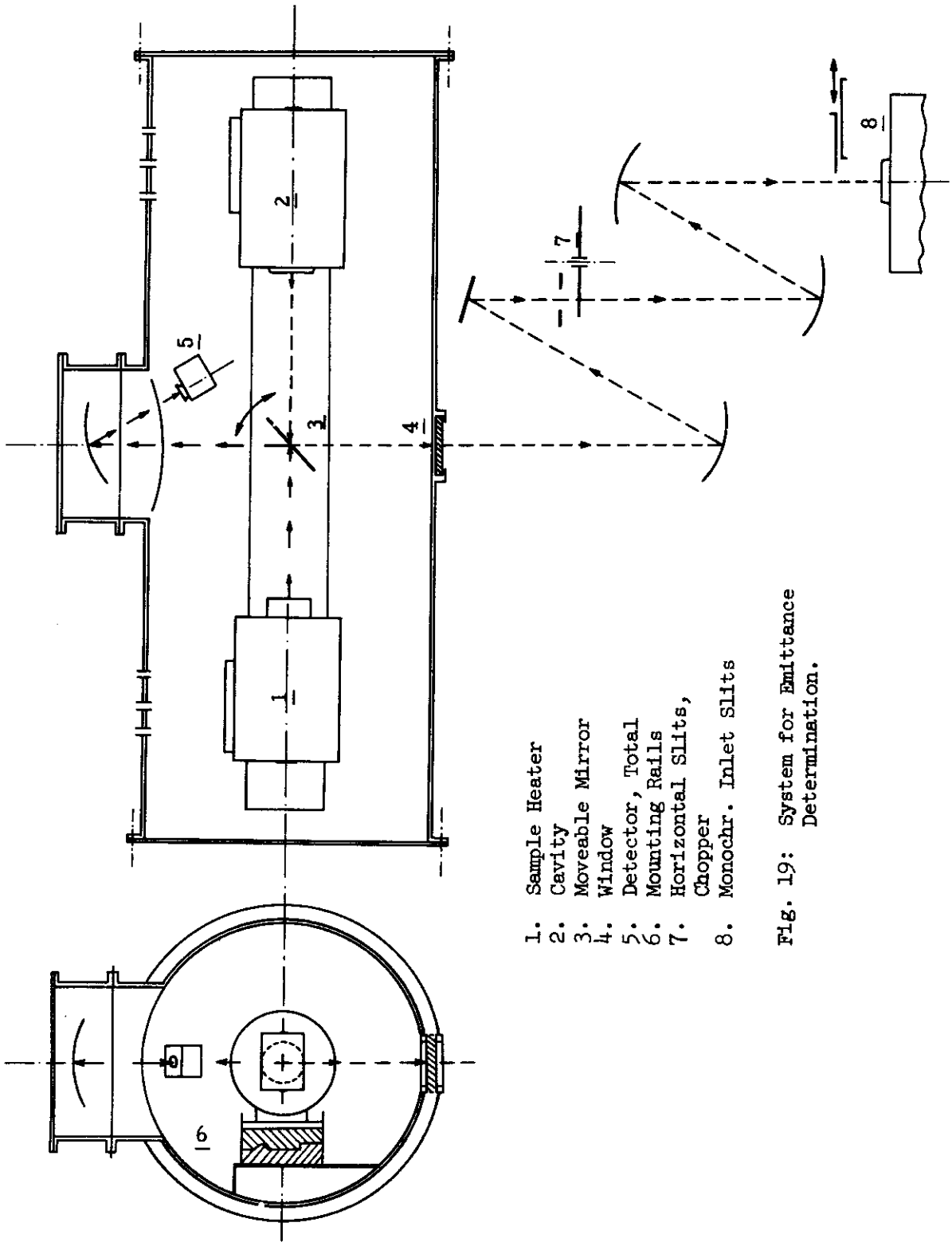

1. Sample Heater
2. Cavity
3. Moveable Mirror
4. Window
5. Detector, Total
6. Mounting Rails
7. Horizontal Slits, Chopper
8. Monochr. Inlet Slits

Fig. 19: System for Emittance Determination.

sample or the cavity, the sighting area being defined by a shield at the detector location. The spherical mirror is located within the tank in a position opposite to that of the window and the spherical mirror receives energy via the moveable plane mirror, properly oriented. The reflectances of the two mirrors are high enough to introduce a negligible error into the determination of total emittance, which determination is considered to be essentially a check on the spectral values that are obtained.

The tank is evacuated by a mechanical vacuum pump and in operation under vacuum the pressures have ranged between one and seven microns. Argon can be introduced, through a silica gel drier, and with inert gas operation the pressure used has been slightly above atmospheric.

4.3 Cavity

The cavity itself is a graphite tube, with an internal diameter of ½ inch and a length of 2-3/4 inches from the orifice to the back, where the thermocouple is located, as shown on Figure 20. The orifice opening is 0.30 inches in diameter. A ceramic tube surrounds the graphite core tube and on this tube there are wound, near the front end, two turns of heavy (80 mil) tungsten wire, while on the remainder of the length of this ceramic tube are contained two separate (40 mil) tungsten heaters. This assembly is cemented and enclosed in a split ceramic tube, which is wound externally with an 80 mil tungsten wire to form the primary heating unit and provide for most of the thermal load. This assembly is encased in another ceramic tube to provide for further temperature reduction and the space between this tube and the jacket is filled with Fiberfrax insulation. The jacket itself contains cooling coils through which water is circulated. A wire suspension, together with the tightness of the Fiberfrax packing, maintains the position of the core tube in the jacket.

In initial operation, at a temperature of about 1800°F, the two turn (80 mil) internal heater was wired in series with the similar external heater and the heat production near the front of the cavity was excessive, so that the temperature at the orifice section was substantially above that at the back of the cavity. Pending the installation of a separate electrical supply for the front heater, that heater was disconnected, so that thereafter the temperature of the orifice section was about 130°F below the temperature at the back of the cavity. Optical pyrometer measurements, together with the magnitude of the emittances observed for certain Inconel samples, lead to

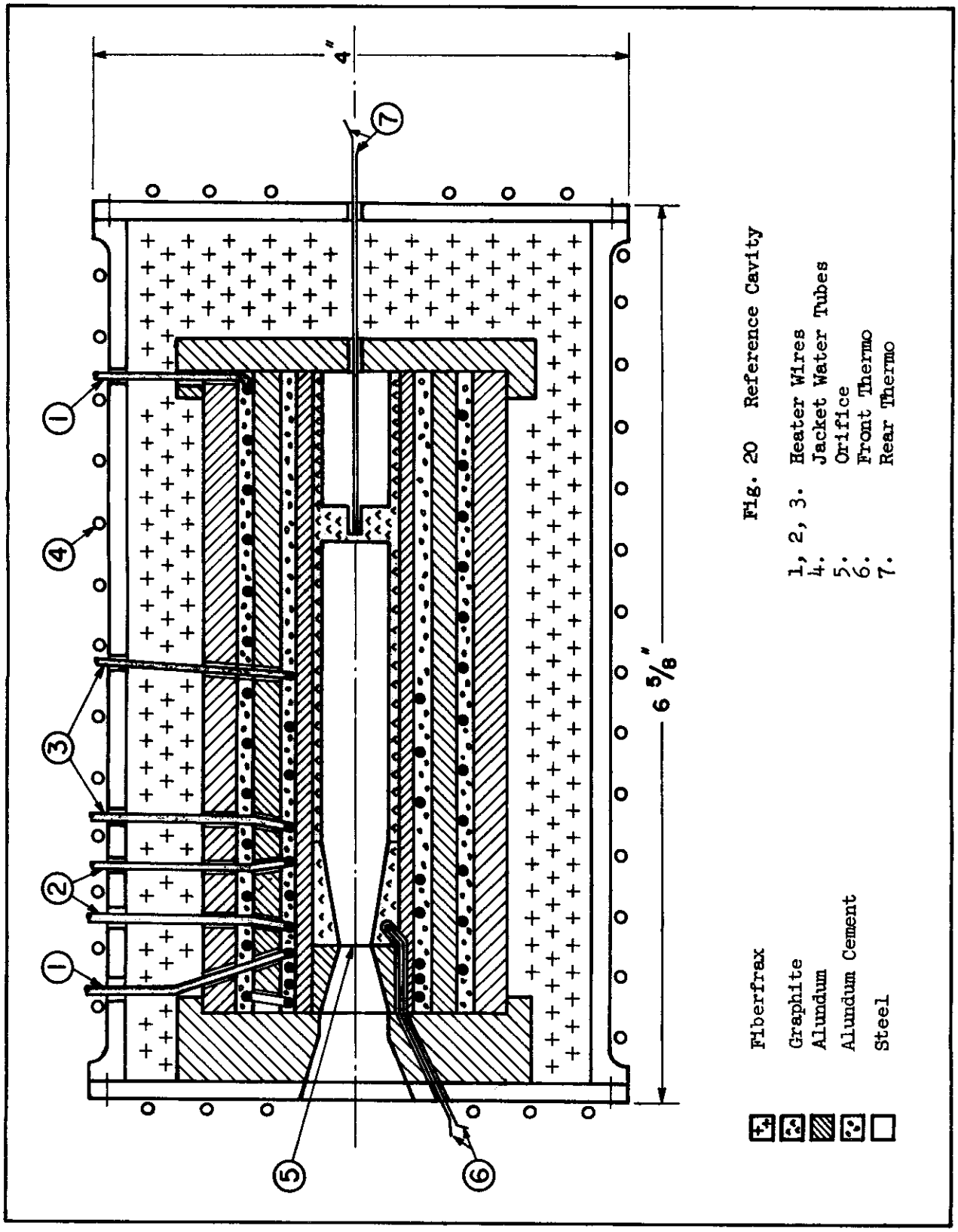

Fig. 20 Reference Cavity

1, 2, 3. Heater Wires
4. Jacket Water Tubes
5. Orifice
6. Front Thermo
7. Rear Thermo

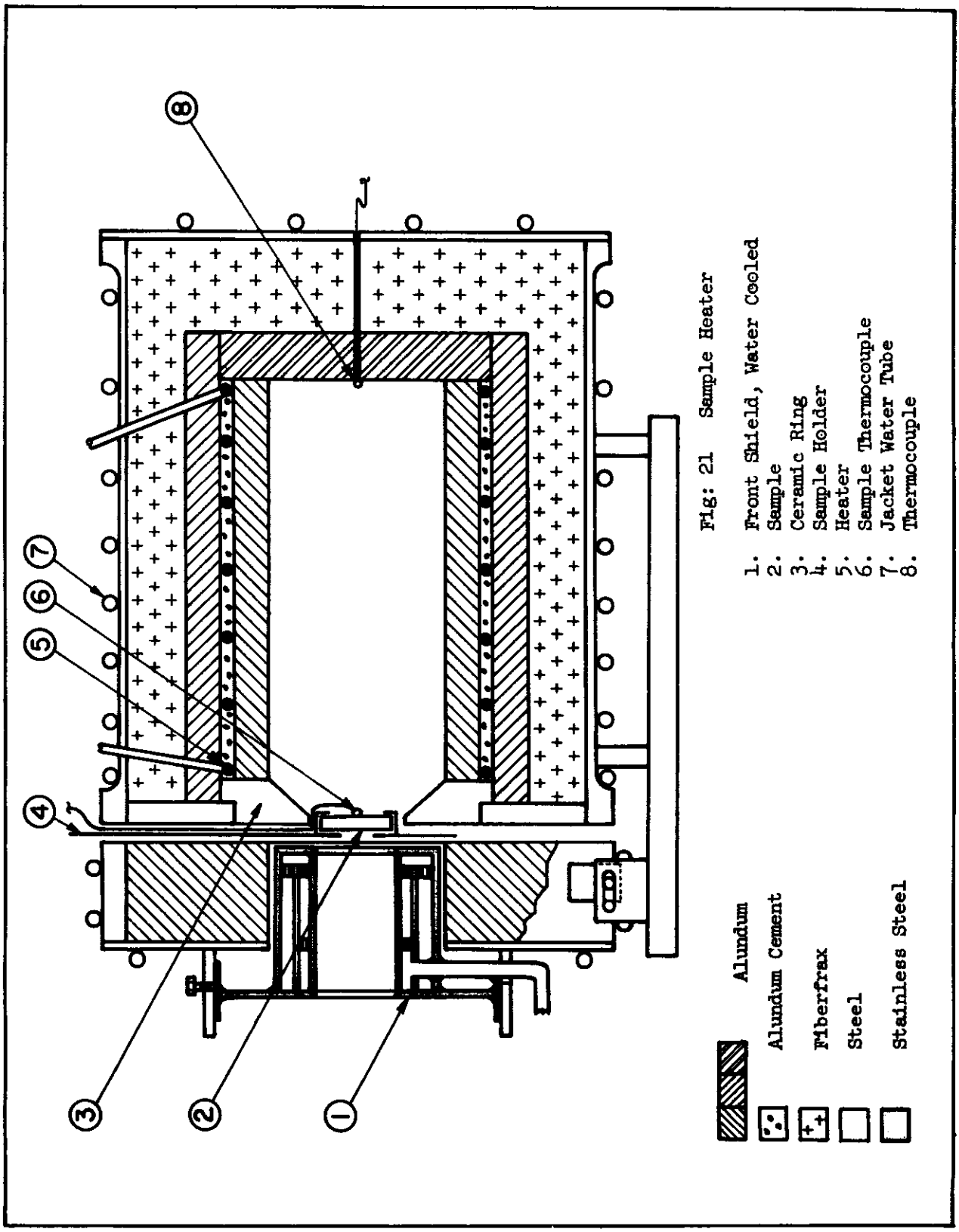

Fig: 21 Sample Heater

1. Front Shield, Water Cooled
2. Sample
3. Ceramic Ring
4. Sample Holder
5. Heater
6. Sample Thermocouple
7. Jacket Water Tube
8. Thermocouple

the conclusion that the sides of the cavity must have been near the temperature indicated by the back thermocouple and that this temperature was indeed close to the black body temperature of the emerging radiation.

4.4 Sample Heater

The decision to provide for sample heating by irradiation of the back of the sample by a furnace, as shown on Figure 21, was based on the desire to retain maximum flexibility with regard to sample thickness and substrate material. A 7/8 inch diameter sample is affixed to a holder made of thin molybdenum sheet, the support being by tabs which project into the furnace opening for registration. A tab projects beyond the edge of the jacket for removal of the sample assembly and this tab supports a ceramic insulator for the wires of the thermocouple that is welded to the heated face of the sample. The front (cooled) face of the molybdenum sample holder contains a central hole, about 0.35 inches in diameter, through which the sample is viewed, and the sample holder then acts as a partial radiation shield on the front of the sample.

The furnace contains a single winding of 80 mil tungsten wire, with general features of insulation and cooling similar to those on the cavity.

A door on the front of the unit provides additional insulation and opens to enable introduction and removal of the sample holder. A water cooled shield, made of stainless steel,is located in the center of the door and its one inch internal diameter is the opening through which the sample is viewed. This internal surface of the shield is honed smooth to produce specular reflection and minimize any reflection of radiation back to the surface of the sample.

4.5 Measurement of Spectral Emittance

The emittance is deduced from the responses of the thermocouple detector in the monochromator, when the cavity is viewed and when the sample is viewed, together with the temperatures inferred from the thermocouples on the sample in the cavity. In the following discussion it is assumed that the temperatures are correct and that the cavity is indeed black, though obvious errors can arise from these sources also. The detector response is assumed to be linearly proportional to the difference between the energy entering the monochromator with the chopper closed, and the constant of proportionality used here includes, with other factors, the angle factor of the energy stream at the

sample and the transmissivity of the window in the tank.

Of that energy reaching the detector from the surface of the sample as a result of reflection therefrom, one component arises from interreflection between sample and window. Since the window reflection is specular, this is equivalent to the irradiation of the sample by its image in the specular window. The distance between the sample and its image in the window is about 20 inches and thus a negligible amount of energy is returned by this reflection.

A more important contribution to the radiosity of the sample surface arises from the diffuse admission $_{m}E_{m}$ of the mirror and of the window $\epsilon_{w}E_{w}$, the latter reaching the sample surface by way of the mirror which in this connection is assumed to be of unity reflectance. With A the area of the window, the irradiation of the sample is $\epsilon_{w}AE_{w}F_{ws}$, or, by reciprocity, $A_{s}E_{w}\epsilon_{w}F_{sw}$, and with diffuse reflection the contribution to the sample radiosity is then $\epsilon_{w}E_{w}F_{sw}$. But $F_{sw} = .004$ and since $E_{w} \ll E_{s}$, this contribution, and the similar contribution from the mirror, is negligibly small. If, however, the reflection of the sample is specular, then the effect is more severe because, in view of the small sample area, practically all of the irradiation is reflected into the cone of observation, for which the angle factor is practically F_{sw}. Thus the addition to the emission from the sample is, in the cone of observation, $\epsilon_{w}E_{w}r_{2}$ due to the emission from the window and $\epsilon_{m}E_{m}r_{2}$ due to emission from the mirror and it turns out that for specular samples of low emittance the emissive powers of the window and mirror must be minimized.

In addition to these components, the sample is irradiated by the surface of the shield, for which the angle factor to the surface is large, and in addition there is a small contribution from the interior of the tank. The temperature of this irradiation is below that of the external surroundings but the ensuing algebra is simplified somewhat by taking the emissive power of that irradiation as E_{o}, the same as that of the external surroundings. Then the contribution to the reflected energy is $r_{2}E_{o}$, and this contribution exists only for a diffuse sample.

A further contribution to the monochromator input arises from direct emission from the mirror, the window, and the two external mirrors, of emissive power, E_{o}, located upstream of the chopper. If the rays of these emissions which do enter the monochromator are traced backward, they impinge on the sample in the viewed area, so that to the first order the effect of these added emissions is identical to an addition of these emissive powers, based on appropriate emissivities of the sample surface or at the cavity.

All of these effects are tabulated in summary to indicate the total contribution to the detector response.

Sample $\epsilon_2 E_2$		Emission	Cavity E_1
negligible		Inter reflection with window	0
$\epsilon_w E_w r_2$	specular sample only	Reflection of window irradiation	0
$\epsilon_m E_m r_2$	specular sample only	Reflection of mirror irradiation	0
$r_2 E_o$	diffuse sample only	Reflection of irradiation from shield and tank interior, $E \approx E_o$	0
$\epsilon_m E_m$		Direct emission from mirror	$\epsilon_m E_m$
$\epsilon_w E_w$		Direct emission from window	$\epsilon_w E_w$
$2\epsilon_m E_o$		Direct emission from external optics	$\epsilon_w E_o$
E_o		Less radiosity of chopper surface	E_o
		Detector Response Proportional to net value	

Thus the ratio of the detector responses for the sight on the sample and for the sight on the cavity is for a diffuse sample

$$\frac{S_2}{S_1} = \frac{\epsilon_2 E_2 + [\epsilon_m E_m + \epsilon_w E_w] + (1-\epsilon_2)E_o + 2\epsilon_m E_o - E_o}{E_1 + [\epsilon_m E_m + \epsilon_w E_w] + 2\epsilon_m E_o - E_o} \qquad 4.1$$

or for a specular sample

$$\frac{S_2}{S_1} = \frac{\epsilon_2 E_2 + (2-\epsilon_2)[\epsilon_m E_m + \epsilon_w E_w] + 2\epsilon_m E_o - E_o}{E_1 + [\epsilon_m E_m + \epsilon_w E_w] + 2\epsilon_m E_o - E_o} \qquad 4.2$$

Now the emissive power of the moveable mirror and of the window are not known and it is necessary to decide on the limits of accuracy of the emittance which is evaluated according to the relation

$$\epsilon_2 = \frac{S_2 (E_1 - E_o)}{S_1 (E_2 - E_o)} \qquad 4.3$$

The comparison is indirect because the emissive powers of the window and mirror are actually not known, but the assumption of values much higher than they are expected to be indicates that the emittance of the sample can be determined with negligible error from Equation 4.3 when the sample is diffuse and when its emittance is greater than 0.20. When the emittance of the sample is below this value, and particularly when the sample is specular, the factor by which Equation 4.3 must be multiplied to specify the emittance as given by Equation 4.2 becomes more important. The factor is:

$$\frac{\epsilon_2 \left[1 + \frac{2\epsilon_m E_o + [\epsilon_m E_m + \epsilon_w E_w]}{[E_1 - E_o]} \right]}{\epsilon_2 + \frac{2\epsilon_m E_o + (2-\epsilon_2)[\epsilon_m E_m + \epsilon_w E_w] - (1-\epsilon_2) E_o}{[E_2 - E_o]}} \qquad 4.4$$

Clearly, the second term in the denominator must be much less than $_2$ if that emittance is to be obtained accurately from Equation 4.3. For very small values of ϵ_2 that term is, for $\epsilon_m = 0.10$, $\epsilon_w = 0.10$, approximately

$$0.20 \frac{E_w}{E_2} + 0.20 \frac{E_w}{E_2} - 0.80 \frac{E_o}{E_2} \qquad 4.5$$

With mirror and window temperatures of 200°F, greater than they are expected to be, sample at 1500°F and surroundings at 70°F, this group has the value of 0.01 at 15 microns. This indicates, correctly, that difficulties will arise with metallic samples,

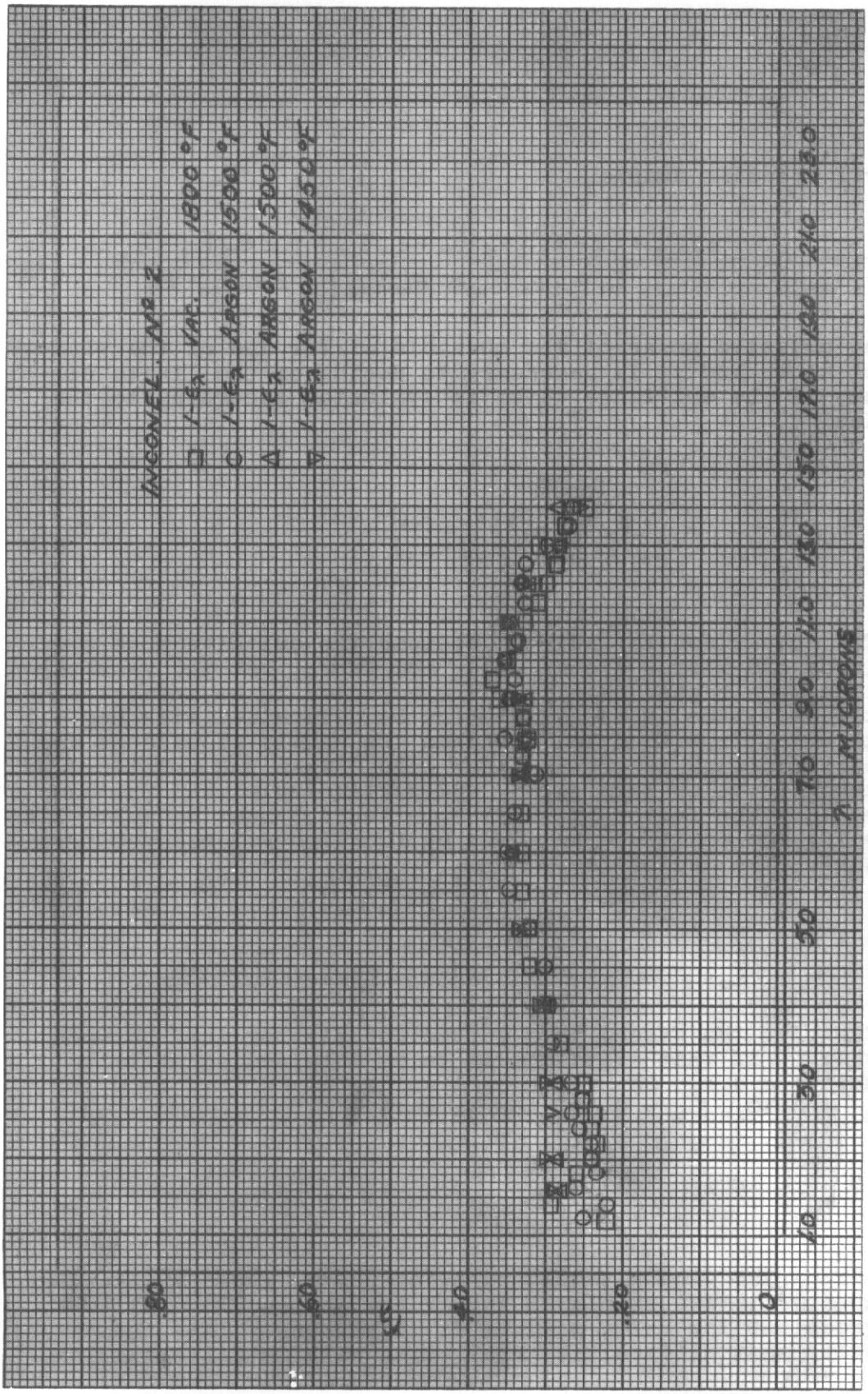

Fig. 22: Spectral Reflectance of Oxidized Inconel Obtained as Emittance in Vacuum and Argon at Temperature Indicated.

the emittance of which may be less than 0.10 at long wave lengths. But the situation in this case is more complicated, and errors arise also from effects associated with the transmittance of the window, which must also be accounted for if the emittance of specular surfaces that are poor emitters is to be evaluated correctly.

4.6 Preliminary Results

The initial operation of this system was with an oxidized Inconel sample, not identical to but similar to that for which reflectances are shown on Figure 1. Temperatures ranged from 1500°F to 1800°F, with vacuum and with argon, and the emittances that were obtained are shown on Figure 22. A high degree of consistency is realized at wave lengths above 2 microns, and the results agree generally with those shown on Figure 1. The considerations of the preceding section indicate that little error would be expected in these emittances, obtained from Equation 4.3, because of the high emittance of the material, but it is of interest that no perceptible detector response was obtained when the mirror was placed parallel to the window. This indicates the relatively small value of the contribution of the emission from the mirror and the window to the detector response.

V

VARIOUS ADDITIONAL RESULTS

5.1 Introduction

A substantial amount of information on the relation between spectral reflectance, spectral emittance, and total emittance was obtained in connection with the examination of certain coated samples prepared by the Chance-Vought Company and some of these results were used in Section 2.3. A more complete set of results is presented in this section and this shows also the variability in the radiation properties that can occur with individual samples even when they are carefully prepared with the objective of complete similarity.

Spectral reflectance results are presented for certain coated molybdenum samples for which a complete evaluation was not possible because of difficulties with substrate oxidation. The few values of total emittance that were obtained do agree with what is predicted from the reflectance at room temperature.

Results are indicated for the total normal emittance of platinum - 13% rhodium and of a sample of Rene 41, as measured in connection with a program of comparison of emittance determination by various techniques.

5.2 Chance-Vought Coated Samples

In February 1961 there were transmitted from the Chance-Vought Company samples of three types of coated metallic samples, designated as Vought II and IX, Vought II and IX with flame sprayed TiO_2, and Vought II plus ferroboron. These were provided in the form of 7/8 inch diameter discs for reflectance determination, 1-7/8 inch diameter discs for spectral emittance determination, and $4\frac{1}{2}$ x $4\frac{1}{2}$" squares for total emittance determination. On one of each of the latter two types of samples, thermocouples were attached and coated before delivery in an attempt to seal the point of thermocouple attachment and thus prevent the separation that can be caused by oxidation of the metal substrate.

Results were obtained, though not for exactly the same spectral range in all cases, for the spectral reflectance at room temperature from the heated cavity and integrating sphere systems, and for spectral emittance at temperature of the order of 1200°F in the spectral emittance stand. Comparisons of some of these results have already been made in Section 2.3. In

addition, total emittance determinations were made in the electrically heated stand for temperatures below 1800°F and with the gas fired stand in the range from 1800°F to 2800°F.

The determinations of both spectral and total emittance were affected seriously by the failure of many of the carefully prepared thermocouples, caused by separation of the tab to which the thermocouple was attached or by oxidation through the coating causing separation of the thermocouples. Oxidation difficulties, either on the original thermocouples or on those attached during the tests by breaking the coating and welding to the substrate, limited the sample temperature to 1200°F for emittance determinations. Table II is the history of thermocouple life and use on these samples. Section 5.3, 5.4, 5.5, present the results for these materials. With slight additions these results are identical to those of the letter report to the Aeronautical Systems Division, Attn:ASRCPT-1, dated June 22, 1961.

Table III History of Chance-Vought Thermocouples

Reflectance Samples, 7/8" D

Material	Number of Samples	Thermocouple
II & IX	2	None
II & IX + TiO_2	2	None
II + Ferroboron	2	None

Spectral Emittance Samples, 1-7/8" D

Material	Thermocouple	Attached By	Remarks
II + IX	Ch-Al	C.V.	Front thermocouple broken on unwrapping, back thermocouple failed before operating temperature attained. No runs made with this sample
II + IX	Ch-Al (40-gauge wire)	U.C.	Welded to base metal at back of sample. Useable below 1200°F

Material	Thermocouple	Attached By	Remarks
II + IX + TiO_2	Ch-Al	C.V.	Wire brittle near ceramic attachment and broke easily. Back thermocouple re-welded twice. Data obtained.
II + IX + TiO_2	Ch-Al (40-gauge wire)	U.C.	Welded to base metal at back of sample. Useable below 1200°F.
II + Ferroboron	Ch-Al	C.V.	Front thermocouple separated on un-packing, back thermo-couple satisfactory at 1200°F.
II + Ferroboron	Ch-Al (40-gauge wire)	U.C.	Welded to base metal at back of sample. Useable below 1200°F.
Total Emittance Samples, 4-1/2" x 4-1/2"			
II + IX	Ch-Al	C.V.	Wire broke at ceramic upon removal from package. Not re-pairable.
II + IX	Ch-Al	U.C.	Welded to base metal at back of sample. Useable to 1200°F.
II + IX	Pt-Pt 13% Rh	C.V.	Temperature indica-tion apparently satisfactory up to 2500°F. Above this, readings were low and partial separation of ceramic apparently occurred. The ceramic separated easily at the end of the experiment.

Total Emittance Samples, 4-1/2" x 4-1/2"

Material	Thermocouple	Attached By	Remarks
II + IX + TiO_2	Ch-Al	C.V.	Thermocouple failed at 1300°F, readings at lower temperatures appear to be low due to possible separation of ceramic.
II + IX + TiO_2	Ch-Al (28-gauge wire)	U.C.	Welded to base metal at back of sample. Useable to 1200°F.
II + IX + TiO_2	Pt-Pt 13% Rh	C.V.	Ceramic attachment separated upon installation in apparatus. Optical pyrometer used exclusively.
II + Ferroboron	Ch-Al	C.V.	Thermocouple failed at 1300°F. Previous readings low; indicated partial separation of ceramic, 28 gauge Ch-Al thermocouple rewelded on back by U.C.
II plus Ferroboron	Ch-Al (28-gauge wire)	U.C.	Welded to base metal at back of sample. Useable to 1200°F.
II + Ferroboron	Pt-Pt 13% Rh	C.V.	Satisfactory up to 2500°F after which readings became low. Ceramic separated after removal from apparatus.

5.3 Vought II and IX

Spectral Reflectance

The results obtained from the two spectral reflectance samples with the sample at room temperature are shown on the upper part of Figure 23 and these reveal good correspondence between the two samples and also between the results obtained from the heated cavity and from the DK-2 reflectometer.

Figure 6 contains comparable reflectance results obtained from a sample cut from the 1-7/8 inch sample after the spectral emittance determinations, and these results are similar to those on Figure 23. Additional ageing at higher temperatures does produce changes in the reflectance, as shown by the curve on Figure 6 and by the results on Figure 24, which presents the results obtained from reflectance sample No. 2 after a succession of ageing periods at 2000°F, in air. Some of the increase in reflectance shown there is attributed to the presence of $Mo0_3$, and some of the reflectance minima, such as the one at 3 microns, appear to be due to absorption maxima of $Mo0_3$. Figure 23 also contains the reflectances measured on a sample cut from the $4\frac{1}{2}$" x $4\frac{1}{2}$" emittance sample after operation at 2800°F and the increased reflectance is similar to that indicated on Figure 24 as the consequence of ageing.

Spectral Emittance

Values are shown on Figure 23, as obtained at 1200°F. The same values appear on Figure 6, to reveal a general correspondence with the low temperature reflectance except at wave lengths above 10 microns.

Total Normal Emittance

Figure 25 presents the results for total normal emittance and the various points distinguish results obtained with different thermocouples (and also with different samples of this material) as well as those for which temperatures were inferred from optical pyrometer indications combined with the spectral emittance at 0.66 microns that is shown on Figure 23. The results above 2000°F were obtained with the gas fired stand within a period of one hour.

The values found for the total normal emittance show substantial scatter, together with a tendency to diminish as the temperature increases. There is better agreement at the high temperatures with a prediction made from the spectral reflectance

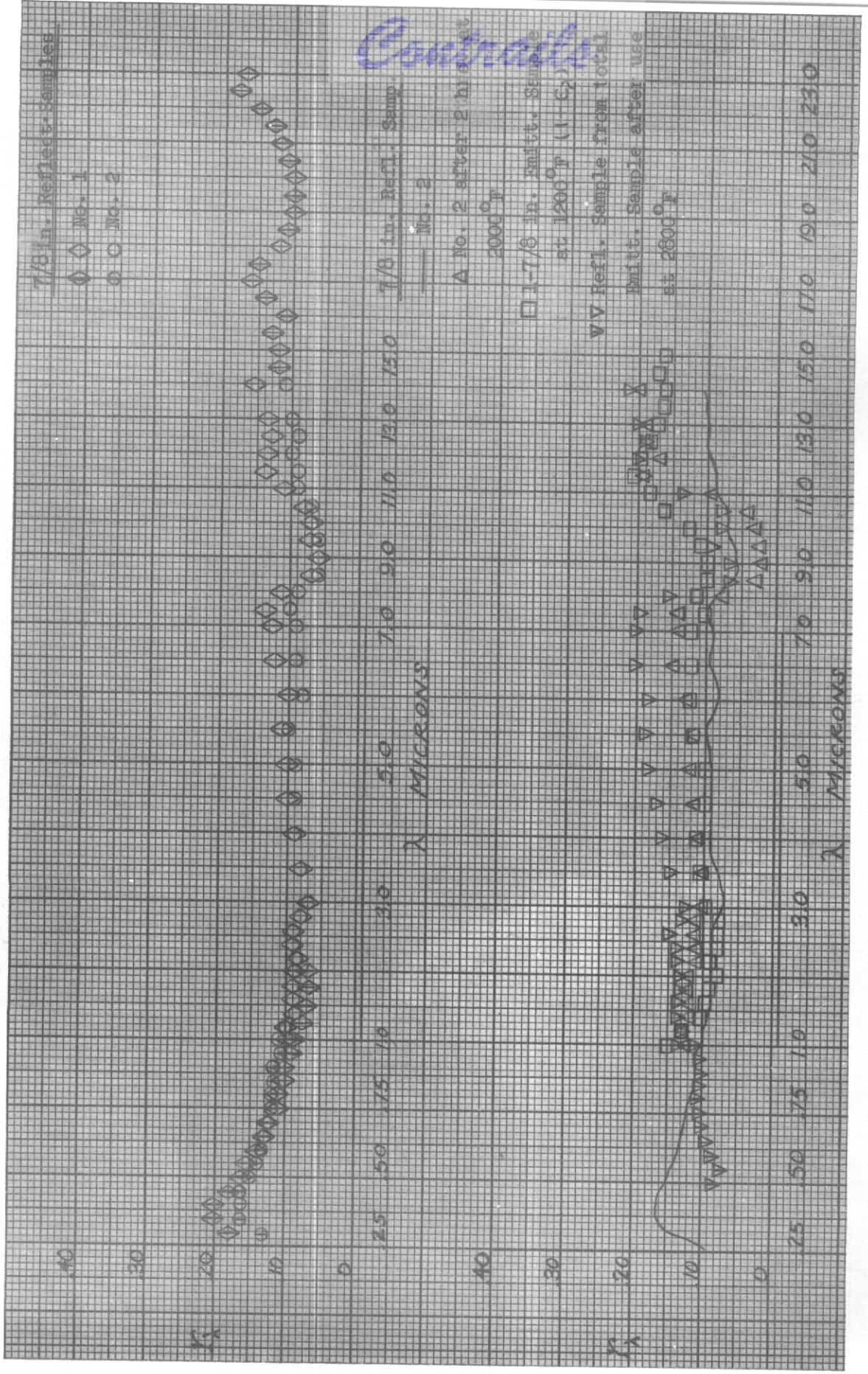

Fig. 23: Spectral Properties, Chance Vought II + IX Coating

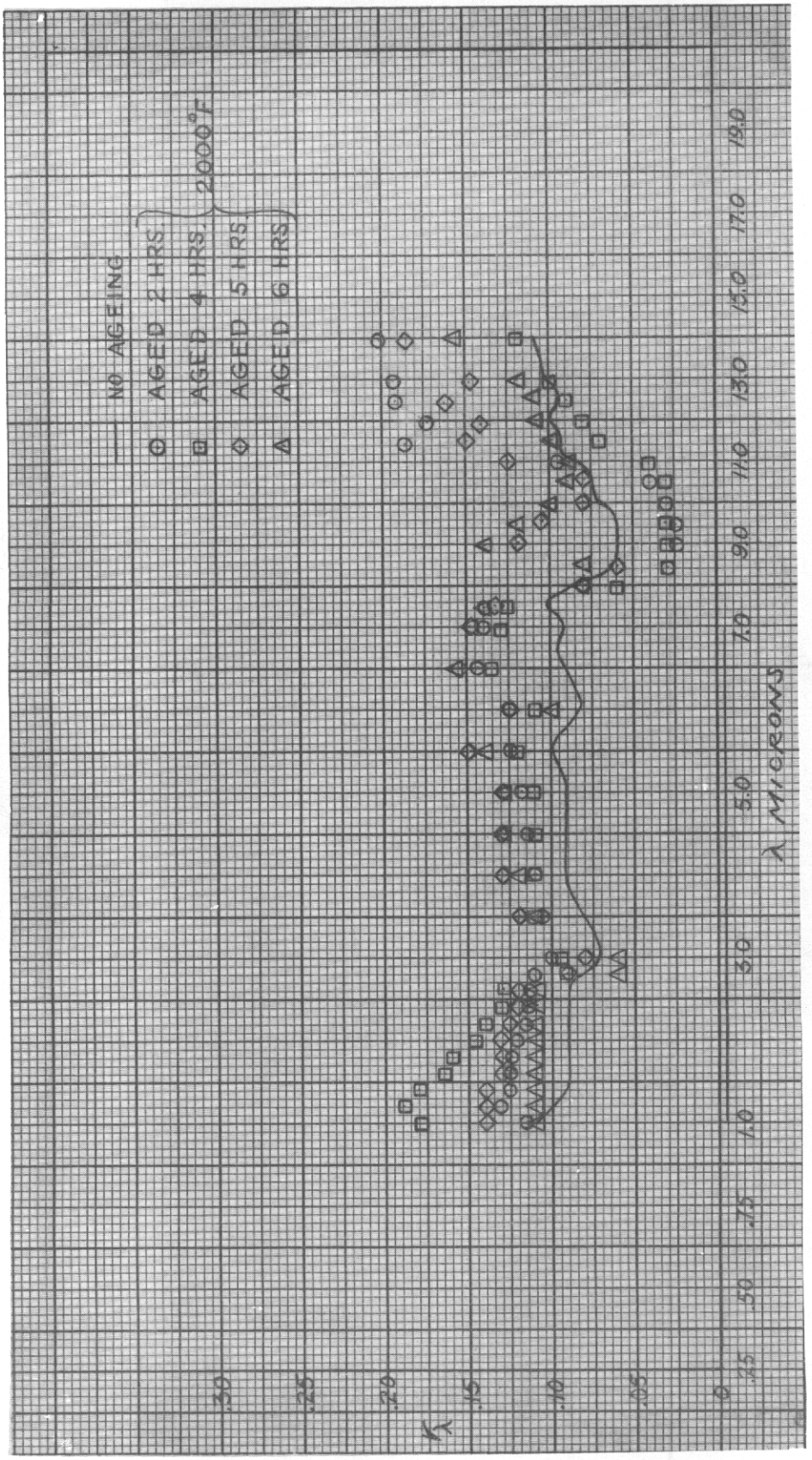

Fig. 24: Effect of Ageing and Spectral Reflectance, Vought II + IX

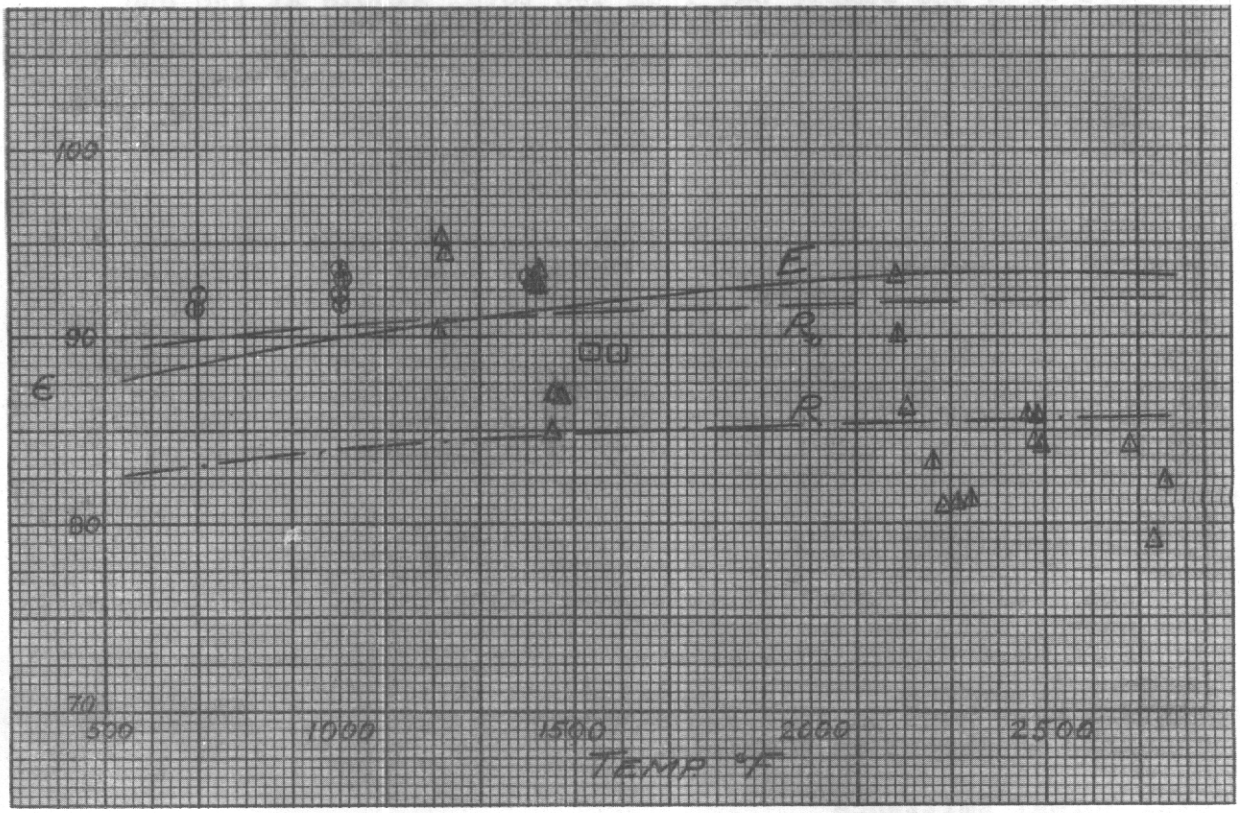

Fig. 25
TOTAL NORMAL EMITTANCE
Chance Vought II+ IX

○ Ch-Al Thermocouple, Back Mounted, U. C.
□ Ch-Al Thermocouple, Chance Vought; Front.
△ Pt-Pt 13% Rh Thermocouple, Chance Vought; Front.
Symbols ◭ ◫ ◑ indicate that emittance calculated from thermocouple indication.
Symbols △ □ ○ indicate that emittance calculated from optical pyrometer indication.
Curves are integrated spectral values.
R_o from original spectral reflectance sample.
R from spectral reflectance sample cut from total emittance sample.
E from spectral emittance results of sample indicated by □ in Fig. 23

measured from the sample cut from the total sample at the end of this operation, but the scatter is so great that a firm conclusion cannot be drawn.

5.4 Vought II Plus Ferroboron

Spectral Reflectance

Different results, as shown on Figure 26, were obtained from the two reflectance samples between 3 and 11 microns; and Figure 6 shows that a third sample again produced different results, being lower in the spectral region. A fourth sample, obtained from the total emittance sample after heating to 2800°F, shows a further alteration of spectral properties, dissimilar to the aging affect revealed on Figure 6. Therefore, these results indicate a substantial difference between samples as well as a pronounced effect of aging.

Spectral Emittance

The value of spectral emittance, obtained at 1200°F, correspond poorly with the spectral reflectances that are shown on Figure 26, but Figure 6 reveals an appreciable improvement in the correspondence when the observations at low and high temperature were made on the same sample with surface conditions as nearly identical as possible.

Total Normal Emittance

Figure 27 contains the results for total normal emittance, with the symbols indicating a distinction between samples as well as between the thermocouples affixed to them. The scatter is again severe, and it is emphasized more by the dual set of points at high temperature, as obtained from the thermocouple and from optical pyrometer readings, the latter being interpreted on the basis of an emittance of 0.90 at 0.66 microns.

The experimental results agree with the predictions made from the observed values of spectral emittance but this correspondence is clouded by the variability observed in different samples of this material. The total emittance decreases slightly as the temperature increases, and this reduction is supported by the effect of aging shown on Figure 6 and by the limiting prediction obtained from the reflectance associated with the total emittance sample after the completion of those observations.

5.5 Vought II and IX Plus Flame Sprayed TiO_2

Spectral Reflectance

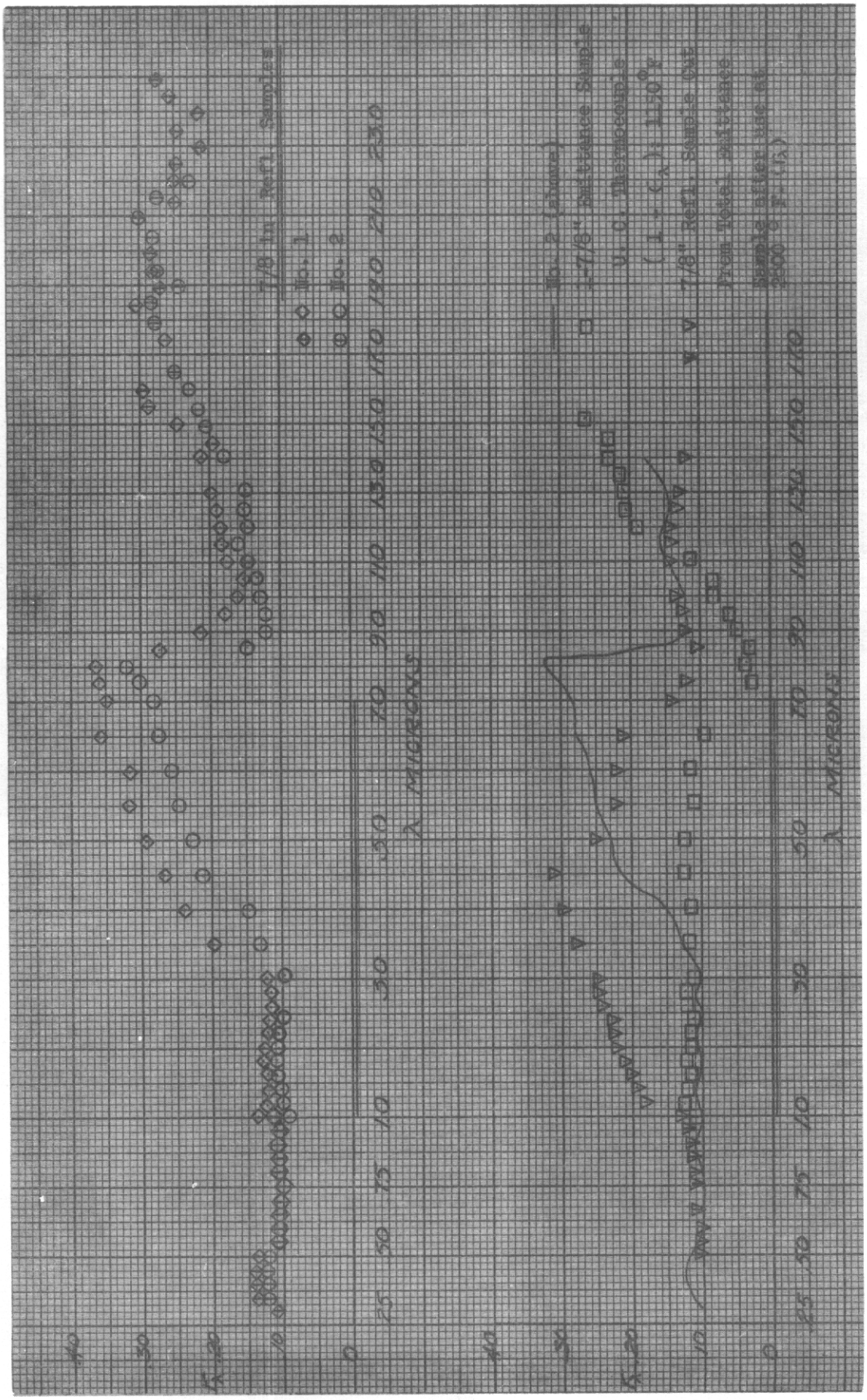

Fig. 26: Spectral Properties, Chance Vought II + Ferroboron

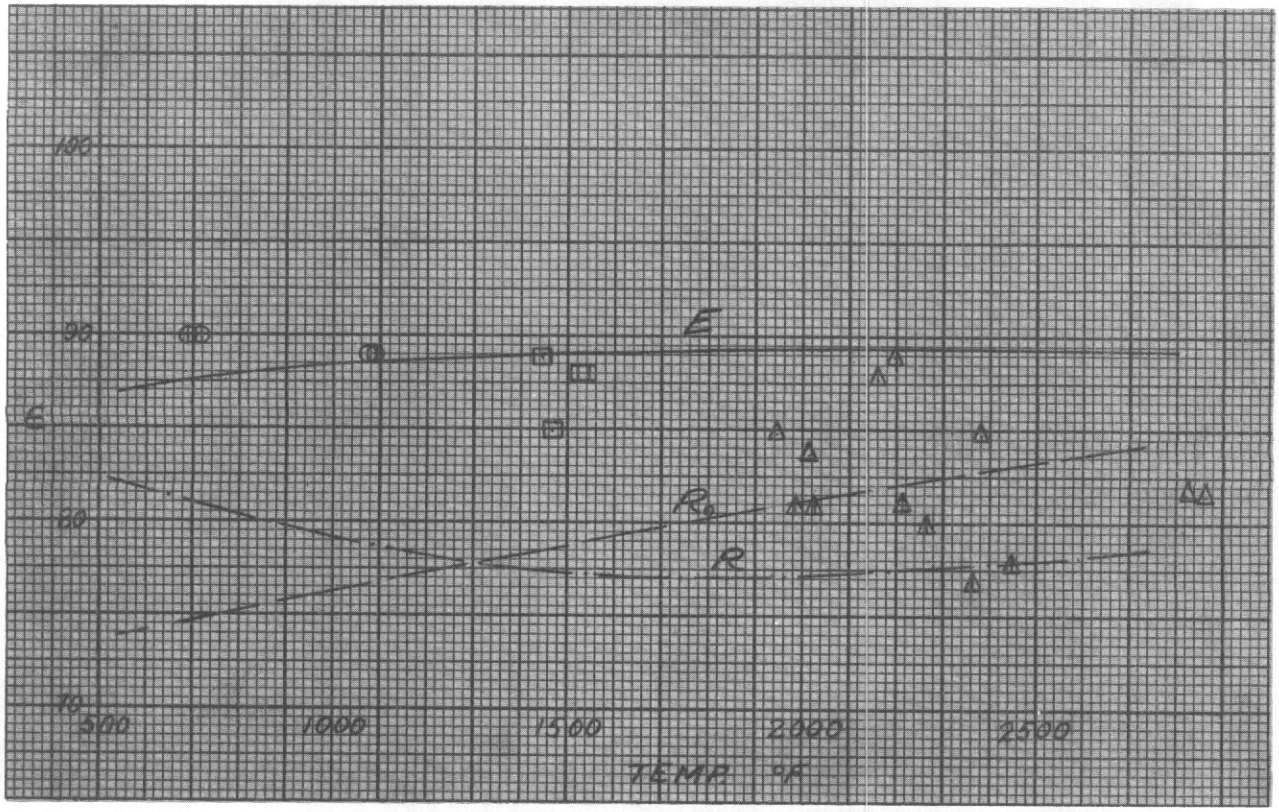

Fig. 27
TOTAL NORMAL EMITTANCE

Chance Vought II + Ferroboron

○ Ch-Al Thermocouple, Back Mounted, U. C.
□ Ch-Al Thermocouple, Chance Vought; Front.
△ Pt-Pt 13% Rh Thermocouple, Chance Vought; Front.
Symbols▲ ▣ ●indicate that emittance calculated from Thermocouple indication.
Symbols△ □ ○indicate that emittance calculated from optical pyrometer indication.
Curves are integrated spectral values.
R_o from original spectral reflectance sample.
R from spectral reflectance sample cut from total emittance sample.
E from spectral emittance results of sample indicated by □ in Fig. 26

Figure 28 shows general agreement between the two 7/8 inch reflectance samples and these reflectances in turn correspond quite well with the spectral emittance measured on one of the emittance samples. Sufficient variability existed in the coating, however, to produce substantially larger spectral emittances in the second emittance sample. The reflectance obtained from this second sample, shown on Figure 6, does generally agree with the spectral emittance values obtained from it. Apparently the TiO_2 coating was thinner on this particular sample resulting in a lower reflectance.

Figure 6 indicates that aging further reduces the reflectance of the sample and this behavior is also evident in the reflectance shown on Figure 28 that was obtained from the total emittance sample after operation at 2800°F, though for this latter sample the original reflectance was apparently nearer that of the high values shown on Figure 28 for the first emittance sample and the reflectance samples.

Spectral Emittance

The difference in the spectral emittances of the two samples, shown on Figure 28, was due to differences in the coatings. The emittance for one of the samples agrees well with the reflectance measured from the 7/8 inch samples while the emittance from the second agrees in magnitude with the reflectance measured later from the same specimen, as indicated on Figure 6.

Total Normal Emittance

Figure 29 contains results which, for temperatures below 1200°F, include some values from a sample with a Chromel-Alumel thermocouple attached by the Chance-Vought Co. These are believed to be high, particularly since the thermocouple attachment separated completely at 1300°F. Similar failure occurred with the platinum-rhodium thermocouple and consequently all high temperature results were obtained from optical pyrometer observations, based on a spectral emittance of 0.77 at 0.66 microns.

In placing this sample on the ceramic support ring of the gas heated emittance stand, molybdenum disilicide powder was placed between the sample and the ceramic surface, this being on the observed side of the sample. When the sample was removed after operation at 2800°F, after a period of about 40 minutes at temperatures in excess of 2100°F at which the results shown on Figure 29 were obtained, all the coating had disappeared from the sample surface that had been in contact with the disilicide, and bare metal appeared there. The 2 inch diameter

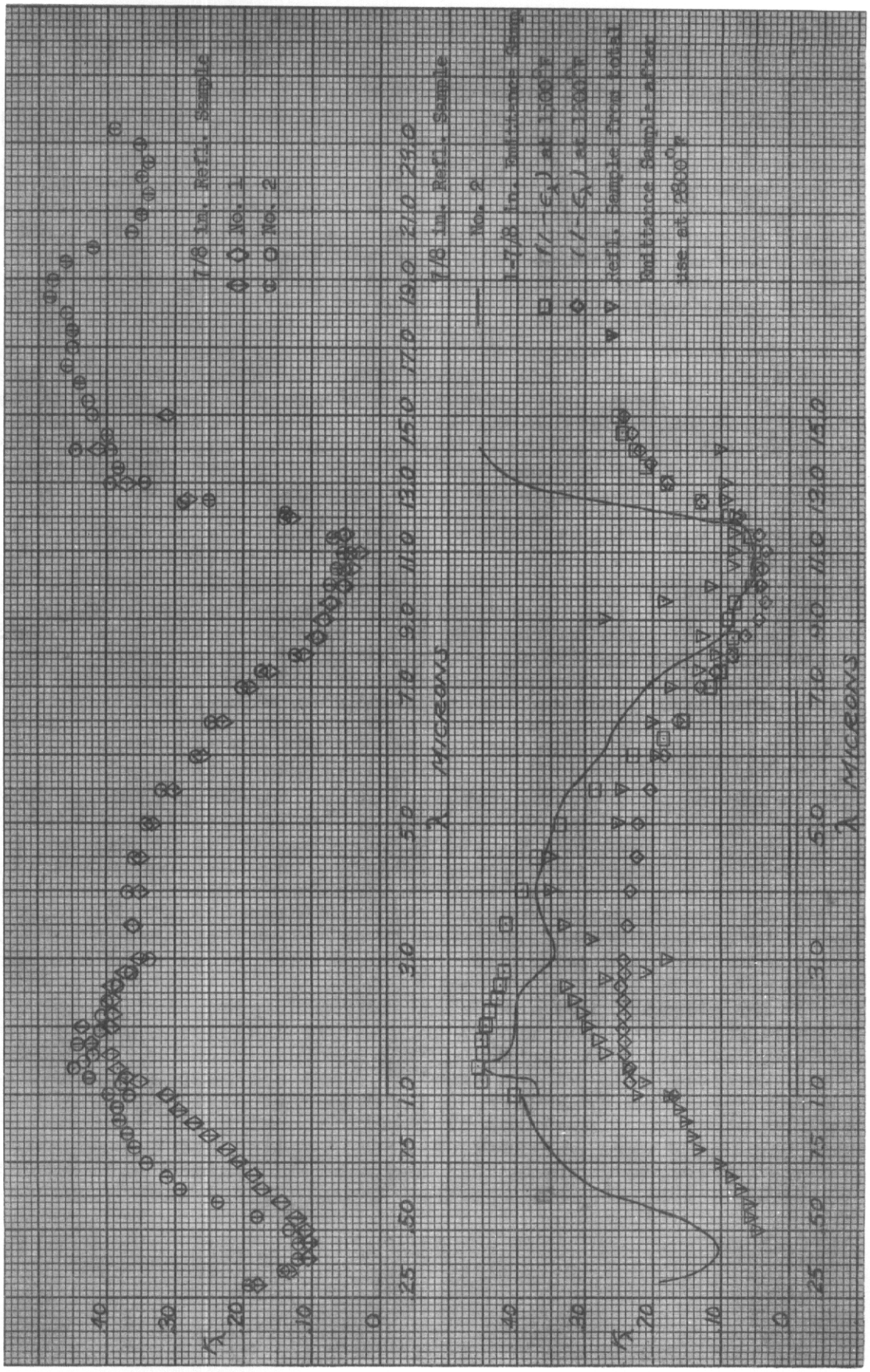

Fig. 28: Spectral Properties, Chance Vought II + IX + TiO_2

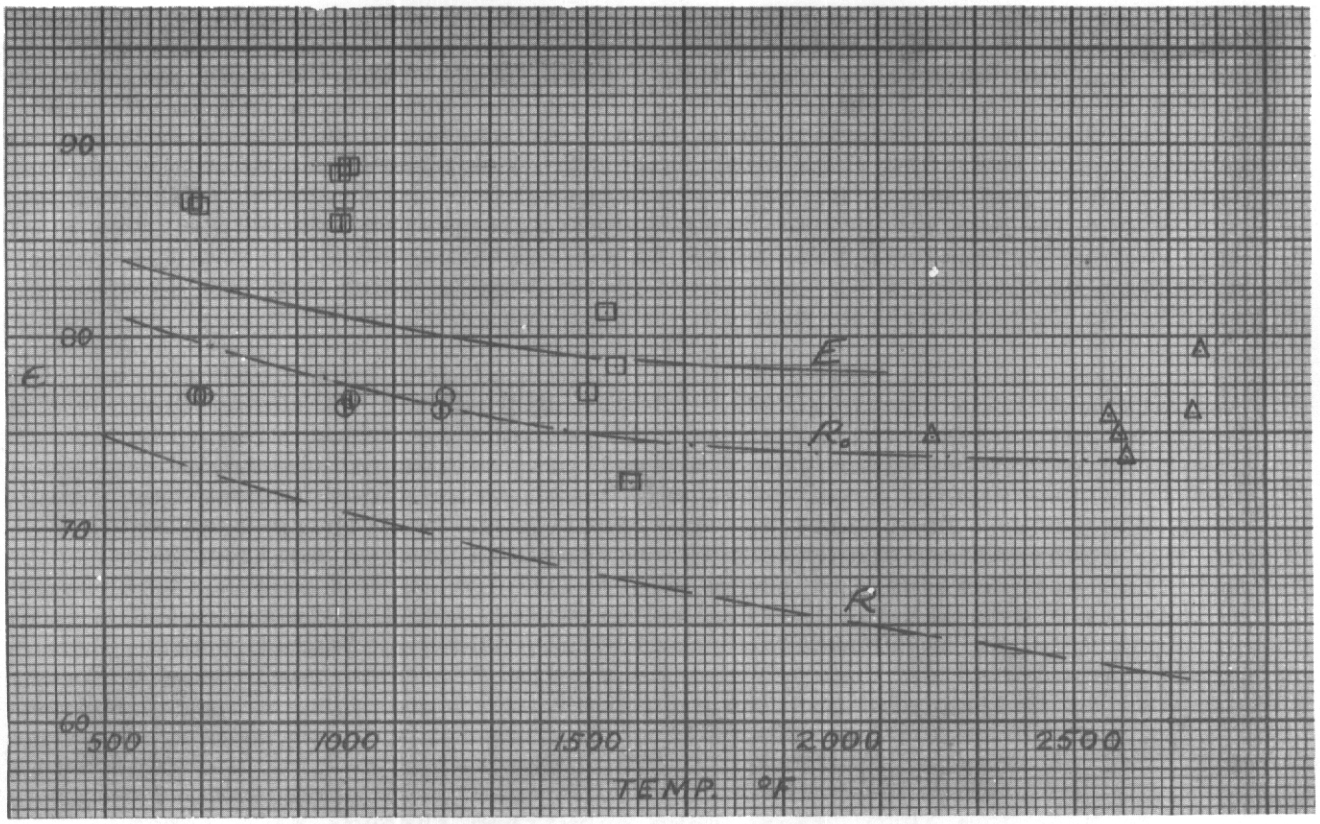

Fig. 29
TOTAL NORMAL EMITTANCE

Chance Vought II+ IX + Flame Sprayed TiO_2

○ Ch-Al Thermocouple, Back Mounted, U. C.
□ Ch-Al Thermocouple, Chance Vought; Front.
△ Pt-Pt 13% Rh Thermocouple, Chance Vought; Front.
Symbols ◭ ◫ ◐ indicate that emittance calculated from Thermocouple indication.
Symbols △ □ ○ indicate that emittance calculated from optical pyrometer indication.
Curves are integrated spectral values.
R_o from original spectral reflectance sample.
R from spectral reflectance sample cut from total emittance sample.
E from spectral emittance results of sample indicated by ◇ in Fig. 28.

center section, where the viewed area was located, was rather black and none of the orange color that originally existed appeared to remain, while the back of the sample that had been exposed to the gas flame had a glazed appearance, still rather orange in color, but otherwise intact. The spectral reflectances obtained from the test surface, after this operation, are shown on Figure 28 and reveal some changes in comparison to the values typical of the original reflectance sample, but the original reflectance of the particular sample used for the total emittance determination was not known.

Figure 29 also contains predictions of the total emittance as obtained from certain spectral emittances and of these the best correspondence with the actual results is associated with the prediction based on the spectral properties of the sample cut from the sample from which the total emittances themselves were measured. Next best is the prediction from the properties of the spectral emittance sample having the larger emittance. But this apparent variation in properties between samples, together with the scatter of the results for total emittance, makes difficult any specific conclusion, though clearly the prediction based on the properties of the 7/8 inch reflectance samples is definitely too low.

5.6 Coated Metals, XP-6789, XP-6790, Chromalloy W-2

In November 1960, there were submitted through WADD three samples of coated metal for the determination of total normal emittance. The metallic substrates contained molybdenum and this led to serious oxidation difficulties at any cut edges and at the point when the coating was broken for thermocouple attachment to the substrate. This latter action was taken in the hope at the time that high temperature paint could be employed to suitably seal this small rupture. The hope was not realized and oxidation occurred, with consequent thermocouple separation. Any further operation, as with an optical pyrometer, was then limited by progressive deterioration at that point, as well as on the cut edges. Total normal emittances were consequently determined only at a few relatively low temperatures.

Spectral reflectances were determined at room temperature from samples cut from the original 6 inch square samples that were supplied and these results are shown on Figure 30. The results for XP 6790 and XP 6789 are almost identical, leading to the inference that the coating was almost identical with these two samples. Also, this is almost true for the Chromalloy W-2 except that the drop in reflectance from its maximum occurs at a higher wave length.

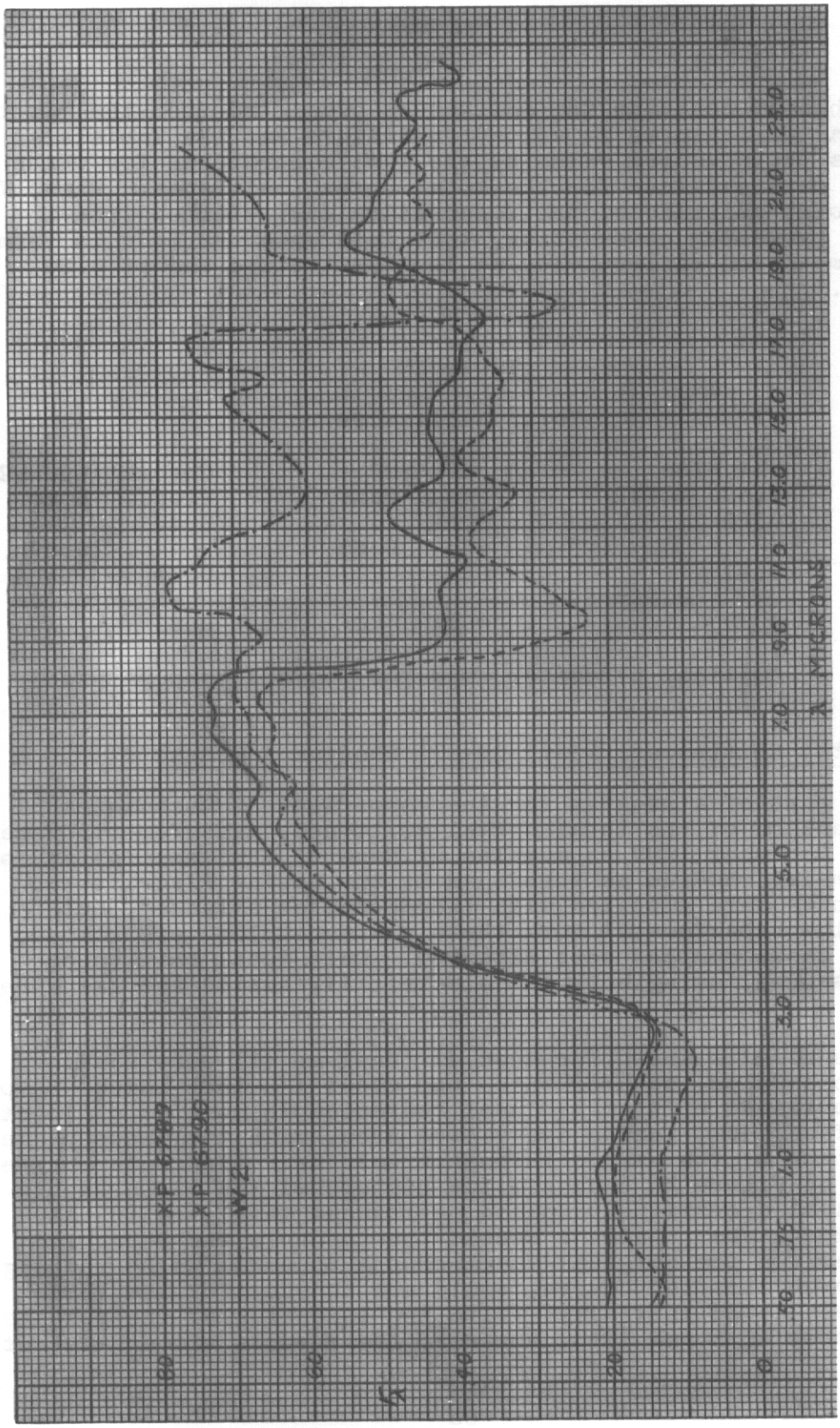

Fig. 30: Spectral Reflectance, Coated XP-6789, 6790, Chromalloy W-2

Table IV contains the emittances predicted from the spectral reflectances measured at a low temperature and the Table also contains the measured value at the few temperatures for which results were obtained for the total normal emittance. When, for these total emittances, the temperature was inferred from an optical pyrometer observation, that inference was made in terms of the measured reflectivity at low temperature and at 0.66 microns.

Table IV

Total Emittances

	XP 6789		XP 6790		Chromalloy W-2	
	Pred.	Meas.	Pred.	Meas.	Pred.	Meas.
540°F	0.45		0.52		0.40	
1380°F				0.65		0.69
1540°F	0.61		0.63		0.60	
1650°F		0.58*				0.70*
2540°F	0.73		0.74		0.73	

*Optical pyrometer used for surface temperature

5.7 Total Emittances, Platinum-13% Rhodium and Rene 41

As part of a program for the comparison of techniques of determination of the total normal emittance, measurements were made in December 1960 on samples of Rene 41 (Unitemp 41) and of platinum-13% rhodium as furnished by the Boeing Aircraft Co. The samples were supplied with thermocouples attached, but during the experimental work these thermocouples were removed and new thermocouples were attached. Only total emittances were measured, using both the electrically heated and gas fired stands.

The results shown for Rene 41 (Unitemp 41) were obtained from two samples, each of which was about 1/8 inch thick. Sample No. 1 contained a Chromel-Alumel thermocouple mounted off center on the face, just inside the viewed area, with the leads passed to the back of the sample through a hole near its center. The symbols on Figure 31 indicate the history of the measurements. The initial operations produced emittances that were low at high temperature. Later a second thermocouple was added and by comparison the original thermocouple appeared to be reading low, though this, of course, would not account for the lower emittances found initially. With the exception of the results of December 16th and 19th, however, the results are consistent

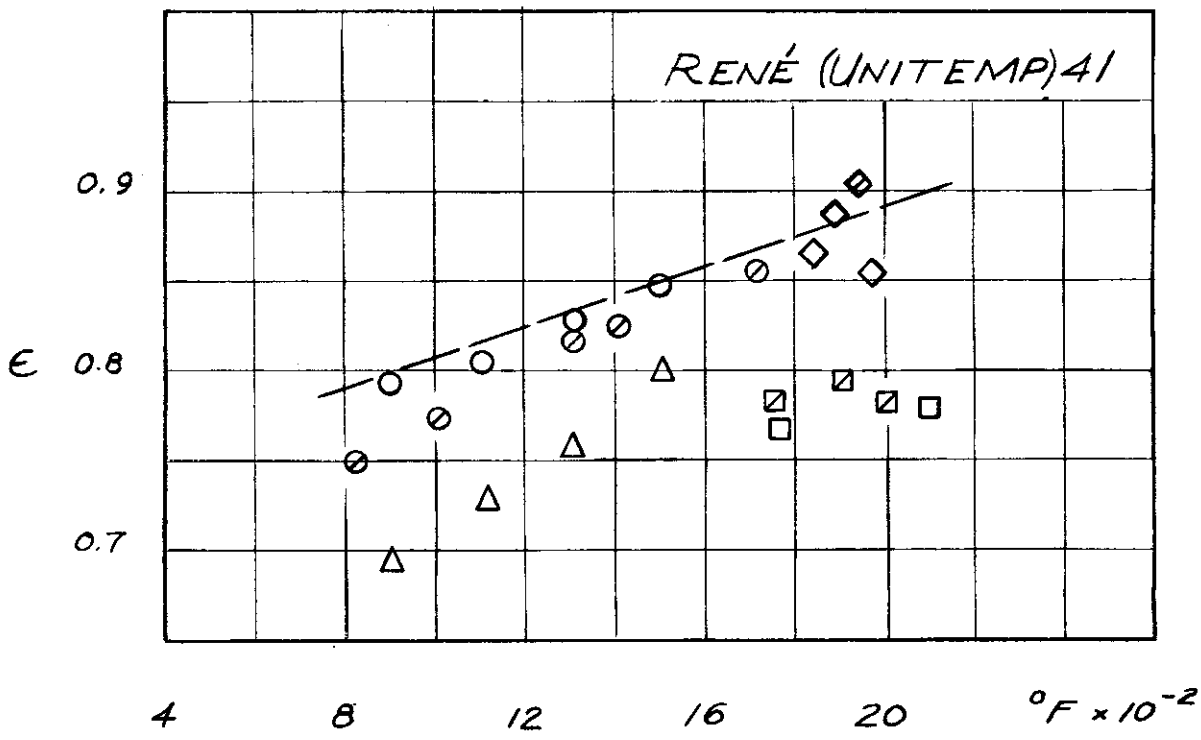

Fig. 31: Total Emittance of René 41

Sample No. 1 Boeing T. C., Ch. Al
- ▨ 12/16 (Gas Std)
- ○ 12/19 (Elec. Std)
- □ 12/21 (Gas Std)
- ⊘ 12/29 & 1/3 (Elec.) U. C. Thermocouple added and used
- ◇ 12/29 (Gas Std) U. C. Thermo.
- ◈ 1/4 (Gas Std) Based on Optical Pyr.

Sample number 2 Boeing T. C. Center Mount

- △ 12/28 (Elec. Std)

The curve indicates the results in Ref. 1

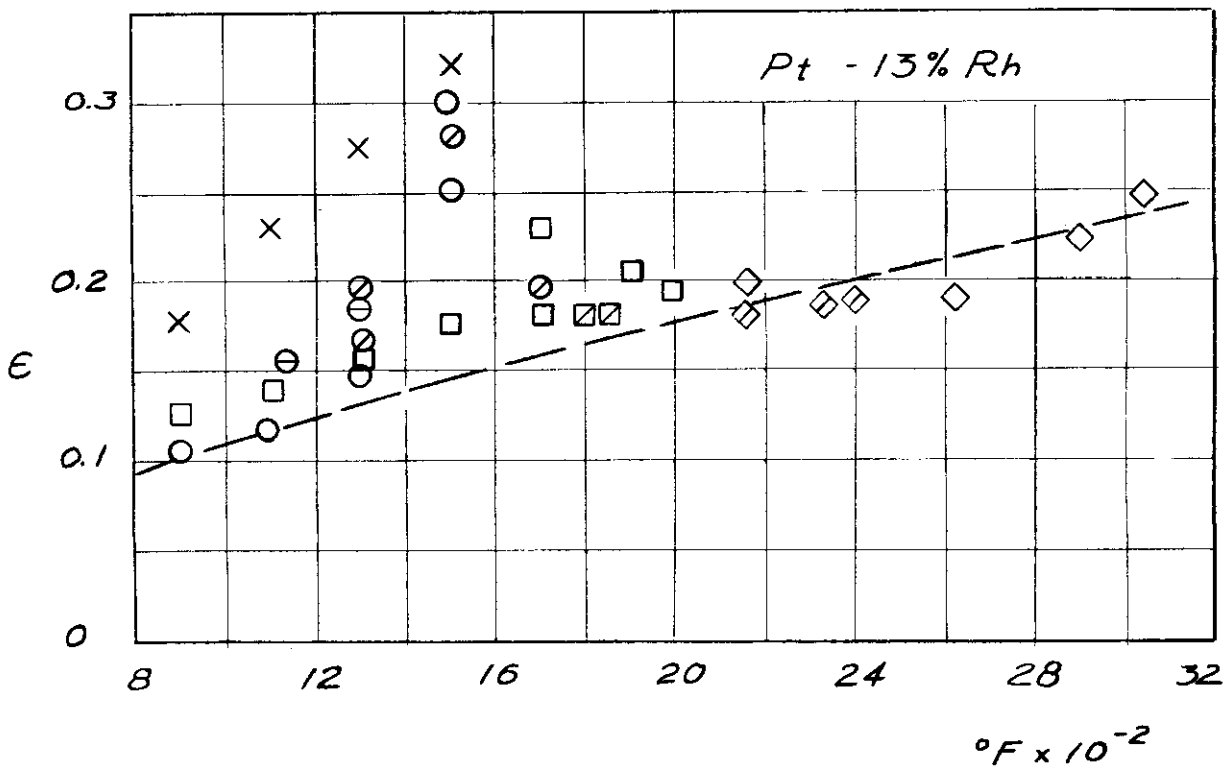

Fig. 32: Total Emittance of Platinum 13% Rhodium Alloy

With Ch-Al Couple (Boeing)
O 12/13 Ø 12/14 θ 12/16
With Pt-Pt 10% Rh Couple (U. C.)
X 12/21 □ 12/22
□ 12/22 ◇ 12/27 ◈ 12/28 (Gas Stand)

The curve is the Hagen-Rubens Law, Eq. 3.1

with the average of earlier measurements on this material, shown by a curve on the Figure. Sample No. 2 was used less extensively, and it gave emittances about 6% lower than the first sample. The difference is attributed to differences in the oxidation rather than to any effect of thermocouple installation.

All the emittances for the sample of platinum-13% rhodium were obtained from a single sample which was provided with a Chromel-Alumel thermocouple, later replaced by a platinum - 10% rhodium thermocouple for operation at high temperature. The results shown on Figure 32 reveal a substantial variation at temperatures below 1900°F, ostensibly due to oxidation of the rhodium, which oxide is eliminated by vaporization at higher temperature. The appearance of the sample also made this distinction, being dull in some of the low temperature operations but becoming bright after operation at high temperature. The "clean" values would then be best given by the minimum values shown on Figure 32.

Because of the applicability as noted in Section 3 of the Hagen-Rubens equation for the prediction of the total normal emittance such a comparison is of interest in relation to the emissivities that are shown on Figure 32. Resistivities of Pt-13% Rh do not appear to be available and the closest information readily at hand is for Pt-10% Rh, which is given only for 20°C, as $\rho_{20} = 20 \times 10^{-6}$ ohm cm and $d\rho/dT = (1.7 \times 10^{-3})\rho_{20}$ Only by the radical assumption that the temperature coefficient given might be used up to very high temperatures is the evaluation of Equation 3.1 possible. The result is the curve of Figure 32. The correspondence with the minimum experimental values is remarkably good.

REFERENCES

1. Seban, R. A. and Rolling, R. E., "Thermal Radiation Properties of Materials", Part I. WADD Technical Report 60-370, Part I, October 1960.

2. Moss, T. S. "Optical Properties of Semi-Conductors", Butterworth's Scientific Publications, London, 1959.

3. Jakob, M. "Heat Transfer," Wiley, 1949, New York.

4. Schmidt, E. and Eckert, E., Forsch. Gebiete Ingenieur., Vol. 6, p. 175, 1935.

5. Abbott, G., Alvares, N., and Parker, W., "Total Normal and Total Hemispherical Emittance of Polished Metals," WADD Technical Report 61-94, April 1961.

6. Pepperhoff, W., "Temperaturstrahlung," D. Steinkopf, 1956, Darmstadt.

7. Givens, M. P., Solid State Physics, Vol. 6, p. 313.

8. Beattie, J. and Conn, G., Philosophical Magazine, Vol. 46, p. 1002, 1955.

9. Roberts, S., Physical Review, Vol. 100, p. 1667, 1956

10. Hurst, C., Proc. Royal Society, Ser. A., Vol. 142, p. 466, 1933.

11. Goldsmith, A., Waterman, T., Hirschborn, H., "Thermophysical Properties of Solid Materials, Elements," WADC TR58-476, Vol. I., 1960.

12. Russell, D. A., "Spectral Reflectance of Rough Surfaces in the Infrared," M.S. Thesis, 1961. University of California at Berkeley.